12. Kamiya,H., Murata-Kamiya,N., Iida,E. and Harashima,H. (2001) Hydrolysis of oxidized nucleotides by the *Escherichia coli* Orf135 protein. *Biochem. Biophys. Res. Commun.*, **288**, 499–502.
13. Sakai,Y., Furuichi,M., Takahashi,M., Mishima,M., Iwai,S., Shirakawa,M. and Nakabeppu,Y. (2002) A molecular basis for the selective recognition of 2-hydroxy-dATP and 8-oxo-dGTP by human MTH1. *J. Biol. Chem.*, **277**, 8579–8587.
14. Fujikawa,K., Kamiya,H., Yakushiji,H., Fujii,Y., Nakabeppu,Y. and Kasai,H. (1999) The oxidized forms of dATP are substrates for the human MutT homologue, the hMTH1 protein. *J. Biol. Chem.*, **274**, 18201–18205.
15. Colussi,C., Parlanti,E., Degan,P., Aquilina,G., Barnes,D., Macpherson,P., Karran,P., Crescenzi,M., Dogliotti,E. and Bignami,M. (2002) The mammalian mismatch repair pathway removes DNA 8-oxodGMP incorporated from the oxidized dNTP pool. *Curr. Biol.*, **12**, 912–918.
16. Russo,M.T., Blasi,M.F., Chiera,F., Fortini,P., Degan,P., Macpherson,P., Furuichi,M., Nakabeppu,Y., Karran,P., Aquilina,G. *et al.* (2004) The oxidized deoxynucleoside triphosphate pool is a significant contributor to genetic instability in mismatch repair-deficient cells. *Mol. Cell. Biol.*, **24**, 465–474.
17. Rai,P., Onder,T.T., Young,J.J., McFaline,J.L., Pang,B., Dedon,P.C. and Weinberg,R.A. (2009) Continuous elimination of oxidized nucleotides is necessary to prevent rapid onset of cellular senescence. *Proc. Natl Acad. Sci. USA*, **106**, 169–174.
18. Tsuzuki,T., Egashira,A., Igarashi,H., Iwakuma,T., Nakatsuru,Y., Tominaga,Y., Kawate,H., Nakao,K., Nakamura,K., Ide,F. *et al.* (2001) Spontaneous tumorigenesis in mice defective in the MTH1 gene encoding 8-oxo-dGTPase. *Proc. Natl Acad. Sci. USA*, **98**, 11456–11461.
19. Hah,S.S., Mundt,J.M., Kim,H.M., Sumbad,R.A., Turteltaub,K.W. and Henderson,P.T. (2007) Measurement of 7,8-dihydro-8-oxo-2'-deoxyguanosine metabolism in MCF-7 cells at low concentrations using accelerator mass spectrometry. *Proc. Natl Acad. Sci. USA*, **104**, 11203–11208.
20. Nohmi,T. (2006) Environmental stress and lesion-bypass DNA polymerases. *Annu. Rev. Microbiol.*, **60**, 231–253.
21. Shimizu,M., Gruz,P., Kamiya,H., Kim,S.R., Pisani,F.M., Masutani,C., Kanke,Y., Harashima,H., Hanaoka,F. and Nohmi,T. (2003) Erroneous incorporation of oxidized DNA precursors by Y-family DNA polymerases. *EMBO Rep.*, **4**, 269–273.
22. Yamada,M., Nunoshiba,T., Shimizu,M., Gruz,P., Kamiya,H., Harashima,H. and Nohmi,T. (2006) Involvement of Y-family DNA polymerases in mutagenesis caused by oxidized nucleotides in *Escherichia coli*. *J. Bacteriol.*, **188**, 4992–4995.
23. Shimizu,M., Gruz,P., Kamiya,H., Masutani,C., Xu,Y., Usui,Y., Sugiyama,H., Harashima,H., Hanaoka,F. and Nohmi,T. (2007) Efficient and erroneous incorporation of oxidized DNA precursors by human DNA polymerase eta. *Biochemistry*, **46**, 5515–5522.
24. Hidaka,K., Yamada,M., Kamiya,H., Masutani,C., Harashima,H., Hanaoka,F. and Nohmi,T. (2008) Specificity of mutations induced by incorporation of oxidized dNTPs into DNA by human DNA polymerase eta. *DNA Repair (Amst.)*, **7**, 497–506.
25. Satou,K., Hori,M., Kawai,K., Kasai,H., Harashima,H. and Kamiya,H. (2009) Involvement of specialized DNA polymerases in mutagenesis by 8-hydroxy-dGTP in human cells. *DNA Repair (Amst.)*, **8**, 637–642.
26. Kouchakdjian,M., Bodepudi,V., Shibutani,S., Eisenberg,M., Johnson,F., Grollman,A.P. and Patel,D.J. (1991) NMR structural studies of the ionizing radiation adduct 7-hydro-8-oxodeoxyguanosine (8-oxo-7H-dG) opposite deoxyadenosine in a DNA duplex. 8-Oxo-7H-dG(syn).dA(anti) alignment at lesion site. *Biochemistry*, **30**, 1403–1412.
27. Oda,Y., Uesugi,S., Ikehara,M., Nishimura,S., Kawase,Y., Ishikawa,H., Inoue,H. and Ohtsuka,E. (1991) NMR studies of a DNA containing 8-hydroxydeoxyguanosine. *Nucleic Acids Res.*, **19**, 1407–1412.
28. Prakash,S., Johnson,R.E. and Prakash,L. (2005) Eukaryotic translesion synthesis DNA polymerases: specificity of structure and function. *Annu. Rev. Biochem.*, **74**, 317–353.
29. Ling,H., Boudsocq,F., Woodgate,R. and Yang,W. (2001) Crystal structure of a Y-family DNA polymerase in action: a mechanism for error-prone and lesion-bypass replication. *Cell*, **107**, 91–102.
30. Alt,A., Lammens,K., Chiocchini,C., Lammens,A., Pieck,J.C., Kuch,D., Hopfner,K.P. and Carell,T. (2007) Bypass of DNA lesions generated during anticancer treatment with cisplatin by DNA polymerase eta. *Science*, **318**, 967–970.
31. Niimi,N., Sassa,A., Katafuchi,A., Gruz,P., Fujimoto,H., Bonala,R.R., Johnson,F., Ohta,T. and Nohmi,T. (2009) The steric gate amino acid tyrosine 112 is required for efficient mismatched-primer extension by human DNA polymerase kappa. *Biochemistry*, **48**, 4239–4246.
32. Anderson,H.J., Vonarx,E.J., Pastushok,L., Nakagawa,M., Katafuchi,A., Gruz,P., Di Rubbo,A., Grice,D.M., Osmond,M.J., Sakamoto,A.N. *et al.* (2008) Arabidopsis thaliana Y-family DNA polymerase eta catalyses translesion synthesis and interacts functionally with PCNA2. *Plant J.*, **55**, 895–908.
33. Trincao,J., Johnson,R.E., Escalante,C.R., Prakash,S., Prakash,L. and Aggarwal,A.K. (2001) Structure of the catalytic core of S. cerevisiae DNA polymerase eta: implications for translesion DNA synthesis. *Mol. Cell*, **8**, 417–426.
34. Lone,S., Townson,S.A., Uljon,S.N., Johnson,R.E., Brahma,A., Nair,D.T., Prakash,S., Prakash,L. and Aggarwal,A.K. (2007) Human DNA polymerase kappa encircles DNA: implications for mismatch extension and lesion bypass. *Mol. Cell*, **25**, 601–614.
35. Sekiguchi,M. and Tsuzuki,T. (2002) Oxidative nucleotide damage: consequences and prevention. *Oncogene*, **21**, 8895–8904.
36. Einolf,H.J. and Guengerich,F.P. (2001) Fidelity of nucleotide insertion at 8-oxo-7,8-dihydroguanine by mammalian DNA polymerase δ. Steady-state and pre-steady-state kinetic analysis. *J. Biol. Chem.*, **276**, 3764–3771.
37. Einolf,H.J., Schnetz-Boutaud,N. and Guengerich,F.P. (1998) Steady-state and pre-steady-state kinetic analysis of 8-oxo-7,8-dihydroguanosine triphosphate incorporation and extension by replicative and repair DNA polymerases. *Biochemistry*, **37**, 13300–13312.
38. de Vega,M. and Salas,M. (2007) A highly conserved tyrosine residue of family B DNA polymerases contributes to dictate translesion synthesis past 8-oxo-7,8-dihydro-2'-deoxyguanosine. *Nucleic Acids Res.*, **35**, 5096–5107.
39. Miller,H., Prasad,R., Wilson,S.H., Johnson,F. and Grollman,A.P. (2000) 8-oxodGTP incorporation by DNA polymerase β is modified by active-site residue Asn279. *Biochemistry*, **39**, 1029–1033.
40. Kamiya,H. and Kasai,H. (1995) Formation of 2-hydroxydeoxyadenosine triphosphate, an oxidatively damaged nucleotide, and its incorporation by DNA polymerases. Steady-state kinetics of the incorporation. *J. Biol. Chem.*, **270**, 19446–19450.
41. Nohmi,T., Kim,S.R. and Yamada,M. (2005) Modulation of oxidative mutagenesis and carcinogenesis by polymorphic forms of human DNA repair enzymes. *Mutat. Res.*, **591**, 60–73.
42. Friedberg,E.C., Wagner,R. and Radman,M. (2002) Specialized DNA polymerases, cellular survival, and the genesis of mutations. *Science*, **296**, 1627–1630.
43. Macpherson,P., Barone,F., Maga,G., Mazzei,F., Karran,P. and Bignami,M. (2005) 8-oxoguanine incorporation into DNA repeats in vitro and mismatch recognition by MutSalpha. *Nucleic Acids Res.*, **33**, 5094–5105.
44. Hardman,R.A., Afshari,C.A. and Barrett,J.C. (2001) Involvement of mammalian MLH1 in the apoptotic response to peroxide-induced oxidative stress. *Cancer Res.*, **61**, 1392–1397.

TOXICOLOGICAL SCIENCES 114(1), 71–78 (2010)
doi:10.1093/toxsci/kfp306
Advance Access publication December 21, 2009

Integration of *In Vivo* Genotoxicity and Short-term Carcinogenicity Assays Using F344 *gpt* Delta Transgenic Rats: *In Vivo* Mutagenicity of 2,4-Diaminotoluene and 2,6-Diaminotoluene Structural Isomers

Naomi Toyoda-Hokaiwado,*[,2] Tomoki Inoue,†[,2] Kenichi Masumura,* Hiroyuki Hayashi,‡ Yuji Kawamura,‡ Yasushi Kurata,‡ Makiko Takamune,* Masami Yamada,* Hisakazu Sanada,§ Takashi Umemura,† Akiyoshi Nishikawa,† and Takehiko Nohmi*[,1]

*Division of Genetics and Mutagenesis and †Division of Pathology, National Institute of Health Sciences, Setagaya-ku, Tokyo 158-8501, Japan; ‡Meiji Seika Kaisha, Ltd, Kohoku-ku, Yokohama, Kanagawa 222-8567, Japan; and §Safety Research Department, Central Research Laboratories, Kaken Pharmaceutical Co., Ltd, Fujieda, Shizuoka 426-8646, Japan

[1] To whom correspondence should be addressed at Division of Genetics and Mutagenesis, 1-18-1 Kamiyoga, Setagaya-ku, Tokyo 158-8501, Japan. Fax: +81-3-3700-2348. E-mail: nohmi@nihs.go.jp.
[2] These authors contributed to this work equally.

Received October 16, 2009; accepted December 15, 2009

An important trend in current toxicology is the replacement, reduction, and refinement of the use of experimental animals (the 3R principle). We propose a model in which *in vivo* genotoxicity and short-term carcinogenicity assays are integrated with F344 *gpt* delta transgenic rats. Using this model, the genotoxicity of chemicals can be identified in target organs using a shuttle vector λ EG10 that carries reporter genes for mutations; short-term carcinogenicity is determined by the formation of glutathione *S*-transferase placenta form (GST-P) foci in the liver. To begin validating this system, we examined the genotoxicity and hepatotoxicity of structural isomers of 2,4-diaminotoluene (2,4-DAT) and 2,6-diaminotoluene (2,6-DAT). Although both compounds are genotoxic in the Ames/*Salmonella* assay, only 2,4-DAT induces tumors in rat livers. Male F344 *gpt* delta rats were fed diet containing 2,4-DAT at doses of 125, 250, or 500 ppm for 13 weeks or 2,6-DAT at a dose of 500 ppm for the same period. The mutation frequencies of base substitutions, mainly at G:C base pairs, were significantly increased in the livers of 2,4-DAT–treated rats at all three doses. In contrast, virtually no induction of genotoxicity was identified in the kidneys of 2,4-DAT–treated rats or in the livers of 2,6-DAT–treated rats. GST-P–positive foci were detected in the livers of rats treated with 2,4-DAT at a dose of 500 ppm but not in those treated with 2,6-DAT. Integrated genotoxicity and short-term carcinogenicity assays may be useful for early identifying genotoxic and nongenotoxic carcinogens in a reduced number of experimental animals.

Key Words: ***gpt* delta transgenic rat; diaminotoluenes; genotoxicity; carcinogenicity; 3R principle.**

Transgenic rodent models have advanced the field of *in vivo* genotoxicity studies (Nohmi and Masumura, 2005; Nohmi *et al.*, 2000). In these models, λ phage DNA carrying reporter genes for mutations are integrated into the chromosomes of transgenic rodents; the phage DNA is retrieved in phage particles by *in vitro* packaging reactions. The rescued phages are introduced into *Escherichia coli* cells, and mutants that were generated in the rodents are selected. With the shuttle vector system, one can examine the mutagenicity of chemicals in any rodent organ or tissues, including germ cells (Eastmond *et al.*, 2009; Hashimoto *et al.*, 2009). In addition, the mutants recovered from the rodents can be characterized by DNA sequencing (Heddle *et al.*, 2000). Transgenic genotoxicity assays are a reliable method for determining whether genotoxicity is involved in chemical carcinogenicity in the target organs of rodents (Thybaud *et al.*, 2003).

In 1996, we developed the novel transgenic mouse *gpt* delta for *in vivo* genotoxicity assays (Nohmi *et al.*, 1996). These mice have approximately 80 copies of λ EG10 DNA at a single site in chromosome 17 of C57 BL/6J mice (Masumura *et al.*, 1999). A feature of this transgenic mouse is that two mutant selections can be performed instead of just one, to identify a wider spectrum of *in vivo* mutations: *gpt* selection to identify point mutations such as base substitutions and frameshift mutations and Spi^- selection to identify deletion mutations. Because of their sensitivity to deletion-type mutations, *gpt* delta mice have been utilized for radiation biology, cancer research, and regulatory toxicology (Aoki *et al.*, 2007; Masumura *et al.*, 2002; Shibata *et al.*, 2009; Xu *et al.*, 2007). In 2003, we established *gpt* delta rats in a Sprague-Dawley (SD) background by introducing λ EG10 DNA into fertilized SD rat eggs (Hayashi *et al.*, 2003). This *gpt* delta rat carries approximately five copies of λ EG10 DNA at a single site in chromosome 4 and is sensitive to induction of point mutations and deletions by benzo[*a*]pyrene and potassium bromate (Hayashi *et al.*, 2003; Umemura *et al.*, 2009).

Here, we report the establishment of *gpt* delta rat in a Fischer 344 background by backcross of SD *gpt* delta rats with F344 rats for 15 generations. We generated F344 *gpt* delta rats because this background is frequently used for 2-year cancer bioassays. In addition, glutathione *S*-transferase placenta form (GST-P)–positive preneoplastic hepatic foci can be analyzed in the rats (Ito *et al.*, 2000). The results of bioassay using GST-P–positive foci show good correlation with those of 2-year cancer bioassay (Ito *et al.*, 2000; Ogiso *et al.*, 1985). Therefore, GST-P–positive foci formation assay was used as short-term carcinogenicity assay in this study. We hypothesized that we could integrate a genotoxicity assay with a short-term carcinogenicity assay utilizing GST-P foci in F344 *gpt* delta rats. This would reduce the number of animals required for both assays and would allow for examination of the relationship between genotoxicity and preneoplastic lesion formation within the same organs and tissues of chemically treated F344 *gpt* delta rats.

To begin validating this system, we examined the *in vivo* genotoxicity and hepatotoxicity of 2,4-diaminotoluene (2,4-DAT) and 2,6-diaminotoluene (2,6-DAT). The first chemical, 2,4-DAT, is used as an intermediate of the production of toluene diisocyanate, which is a monomer for the production of polyurethane, while 2,6-DAT is an intermediate of dyes, rubber chemicals, and various polymers (NTP 1979, 1980). Although both are genotoxic *in vitro* (Cunningham *et al.*, 1989), only 2,4-DAT is carcinogenic in the livers of female mice and male and female rats (NTP, 1979). 2,4-DAT also induces lymphoma in female mice and mammary and subcutaneous tumors in rats. 2,6-DAT is not carcinogenic in mice and rats, regardless of their sex (NTP, 1980). Previous studies with MutaMouse (Kirkland and Beevers, 2006) and Big Blue mouse (Cunningham *et al.*, 1996) indicate that 2,4-DAT is mutagenic in the liver, while 2,6-DAT is not. However, the transgenic mice employed for these studies were males, in which the hepatocarcinogenicity of 2,4-DAT is not observed. In addition, there are no reports on *in vivo* gene mutations in rats. Thus, we decided to examine the *in vivo* genotoxicity of both compounds in the liver, as carcinogenic target organ of 2,4-DAT, and kidney, as non-carcinogenic target, along with immunohistochemical analyses. We chose 500 ppm as the highest dose for both DATs according to the dose used in the National Toxicology Program 2-year cancer bioassay (NTP, 1979, 1980). We treated the rats with chemicals for 13 weeks because this period is customarily used to determine the appropriate doses for 2-year cancer bioassays; furthermore, shorter term treatments (e.g., treatments with potassium bromate for 5 weeks [Umemura *et al.*, 2006]), sometimes do not induce detectable mutations *in vivo*.

MATERIALS AND METHODS

Establishment of F344 gpt delta rats. All the animals were maintained at Japan SLC (Shizuoka, Japan). The F344 *gpt* delta transgenic rat strain was developed by backcrosses of the original SD *gpt* delta transgenic rat with wild-type F344 rats. In brief, male SD *gpt* delta transgenic rat was mated with F344 female rat to produce an F1 generation. Offspring from the F1 generation were mated with F344 rats to yield an F2 generation. All offspring from successive backcrosses were examined for the possession of the *gpt* gene by PCR (Hayashi *et al.*, 2003). After 15 successive backcrosses, identity of the resulting rats to F344 recipient is more than 99.9%. Thus, they were referred to as F344 *gpt* delta rats.

Chemicals. 2,4-DAT (purity 95%) and 2,6-DAT (purity 98%) were purchased from Wako Pure Chemical Industries (Osaka, Japan). Diethylnitrosamine (DEN) was obtained from Sigma-Aldrich Japan (Tokyo, Japan).

Bacterial reverse mutation test (Ames test). The mutagenic activities of 2,4-DAT and 2,6-DAT were assayed in a bacterial reverse mutation assay using *Salmonella typhimurium* tester strains TA98 and YG1024, an *O*-acetyltransferase (OAT)–overexpressing derivative. The test was conducted by the preincubation method (Maron and Ames, 1983) in the presence or the absence of S9 mix. At least two plates were used for each dose, and the mean values of the number of revertants per plate were calculated. Chemicals were dissolved in dimethyl sulfoxide, which was used as the negative control.

Animals, diet, and housing conditions. Male 6-week-old F344 *gpt* delta transgenic rats were obtained from Japan SLC and housed five animals per polycarbonate cage under specific pathogen-free standard laboratory conditions: room temperature, 23°C ± 2°C; relative humidity, 60 ± 5%; with a 12:12-h light-dark cycle; and free access to CRF-1 basal diet (Oriental Yeast Company, Tokyo, Japan) and tap water. After a 1-week acclimation period, the animals were used for the experiments.

Treatments of animals. The protocol for this study was approved by the Animal Care and Utilization Committee of the National Institute of Health Sciences. Thirty male F344 *gpt* delta rats were randomized by weight into six groups. 2,4-DAT and 2,6-DAT were each mixed into Oriental CRF-1 powdered basal diet (Oriental Yeast Company) and stored at 4°C in the dark before use. Starting at 7 weeks of age, the rats were fed diets containing 0, 125, 250, or 500 ppm 2,4-DAT or 500 ppm 2,6-DAT for 13 weeks. There was also a positive control group; these rats were received a once-a-week ip injection of 20 mg/kg body weight DEN for 13 weeks. Parameters monitored included clinical signs, body weight, and food intake. The highest dose of 2,4-DAT was reduced from 500 to 400 ppm at week 9 because the dose at 500 ppm reduced the body weight of rats at week 8. All the surviving animals were killed under ether anesthesia at the end of the experiments. The liver and kidneys were isolated from each animal and were immediately excised, weighed, and cut into 2- to 3-mm-thick slices. The slices were fixed in 10% buffered formalin solution and routinely processed to paraffin blocks for histopathological examination as well as immunohistochemistry. Hematoxylin and eosin-stained tissue preparations cut from the blocks were examined by light microscopy.

Micronucleus assay. At autopsy, 60 μl of peripheral blood was obtained from the tail veins of all animals. The samples were processed according to the instructions supplied with the MicroFlow^{PLUS} kit (Litron, Rochester, NY), fixed in ultra-cold methanol, and stored immediately after fixation at −80°C until flow cytometry analysis was performed. Approximately 20,000 reticulocytes were counted for each sample using Becton-Dickinson FACSCalibur flow cytometer (Franslin Lakes, NJ) to detect the presence of micronuclei (MNs).

Immunohistochemical procedures. Liver sections of 3-μm thickness were treated with rabbit anti-rat GST-P antibody (1:1000; Medical & Biological Laboratories, Nagoya, Japan) and monoclonal mouse anti-Ki67 (MIB-5) antibody (1:50; Dako, Tokyo, Japan) (1:50), respectively. Areas and numbers of GST-P–positive foci larger than 0.1 mm in diameter of the liver sections were quantitatively measured with an image processor for analytical pathology (IPAP-WIN; Sumika Technos Company, Osaka, Japan). To investigate proliferative activity, we counted at least 1000 hepatocyte nuclei in each liver; labeling indices were calculated as the percentage of cells positive for Ki67

staining. The remaining tissues were immediately frozen in liquid nitrogen and stored at −80°C for subsequent mutation assays.

DNA isolation and in vitro packaging of λ phage DNA. High–molecular-weight genomic DNA was extracted from the liver and kidneys using the RecoverEase DNA Isolation kit (Stratagene, La Jolla, CA). λ EG10 phages were rescued using Transpack Packaging Extract (Stratagene).

gpt Mutation assay. The assay was conducted according to previously published methods (Nohmi *et al.*, 1996). All the confirmed *gpt* mutants recovered from the livers were sequenced; identical mutations from the same rat were counted as one mutant. The mutant frequencies of the *gpt* gene (*gpt* MFs) in the liver and kidney were calculated by dividing the number of confirmed 6-thioguanine–resistant colonies by the number of rescued plasmids. DNA sequencing of the *gpt* gene was performed with the BigDye Terminater Cycle Sequencing Ready Reaction (Applied Biosystems, Foster City, CA) on an ABI PRISM 310 Genetic Analyzer (Applied Biosystems).

Spi⁻ assay. The Spi⁻ assay was conducted according to previously published methods (Masumura *et al.*, 2002). To confirm the Spi⁻ phenotype of the candidates, suspensions were spotted on three types of plates on which XL-1 Blue MRA, XL-1 Blue MRA P2, or WL95 P2 strains were spread with soft agar. True Spi⁻ mutants, which made clear plaques on all of the plates, were counted. Spi⁻ mutant lysates were obtained by infecting *E. coli* LE392 with the recovered Spi⁻ mutants. The lysates were used as templates for PCR and sequencing analysis to determine the deleted regions (Masumura *et al.*, 2002). The Spi⁻ mutants were categorized into three classes: one base pair (bp) deletions, deletions of more than 1 bp, and complex mutations. The entire sequence of λ EG10 is available at http://dgm2alpha.nihs.go.jp/default.htm.

Statistical analysis. The statistical significance of the difference in the value of MFs between treated groups and negative controls was analyzed by Student's *t*-test. A p value less than 0.05 denoted the presence of a statistically significant difference. Variances in values for body weight, organ weight, and immunohistochemical data were examined by one-way ANOVA with Dunnett's multiple test to compare the differences between control and treated groups.

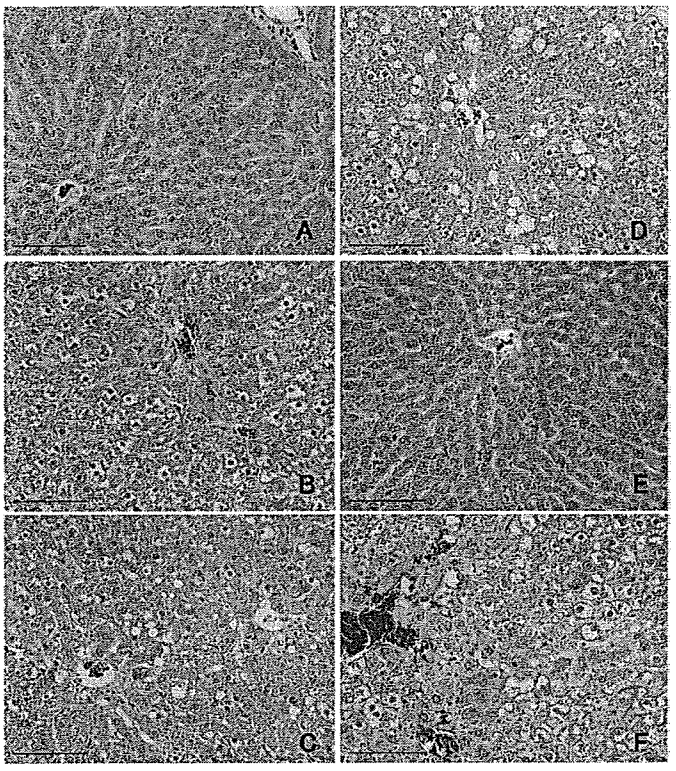

FIG. 1. Histological comparison of rat livers treated with 0 ppm 2,4-DAT (A), 125 ppm 2,4-DAT (B), 250 ppm 2,4-DAT (C), 500 ppm 2,4-DAT (D), 500 ppm 2,6-DAT (E), and DEN (F). Hepatotoxicity was observed in rats administered 2,4-DAT and DEN. Bar = 100 μm.

RESULTS

Dietary Treatment with 2,4-DAT Induced Preneoplastic Lesions in the Livers of F344 gpt Delta Rats

Dietary treatment with 2,4-DAT reduced body weight significantly at all three doses, while dietary treatment with 2,6-DAT did not (Supplementary table 1). Treatments with 2,4-DAT, but not 2,6-DAT, increased the relative weight of the livers and kidneys in a dose-dependent manner. Hypertrophy and vacuolar degeneration of hepatocytes was observed in the livers of rats in the 2,4-DAT treatment groups (Fig. 1). Cell proliferation was significantly enhanced by 2,4-DAT at a dose of 250 ppm but not by treatment with 2,6-DAT or other doses of 2,4-DAT (Table 1). That labeling index was twofold higher compared with that of basal diet group. GST-P–positive foci were induced by treatment with 2,4-DAT at a dose of 250 or 500 ppm and by the positive control treatment with DEN (Table 2). There were significant differences in number of foci and area of foci between rats treated with 2,4-DAT at 500 ppm and those of the basal diet group and between rats treated with DEN and the control group. No histopathological changes were observed in the kidneys of rats that were fed 2,4-DAT or 2,6-DAT. These results suggest that 2,4-DAT, but not 2,6-DAT, induced preneoplastic lesions in the livers of F344 *gpt* delta rats.

Both 2,4-DAT and 2,6-DAT Induced Mutations In Vitro

We confirmed that both 2,4-DAT and 2,6-DAT were mutagenic in *S. typhimurium* strain TA98 in the presence of S9 activation (Fig. 2). Treating cells with either of the DATs in the absence of S9 mix did not produce any increase in the number of revertants per plate. Similar, but less significant, results were obtained with another standard *S. typhimurium* strain TA100 (Supplementary table 2). These observations suggest that DAT metabolites were responsible for the mutagenic effects. To explore the metabolic activation pathways *in vitro*, we employed strain YG1024, which overproduces OAT, a phase II enzyme. Strain YG1024 detects frameshift mutations because it was derived from strain TA98 (Watanabe *et al.*, 1994). As shown in Figure 2, YG1024 exhibited enhanced sensitivity to the mutagenicity of both 2,4-DAT and 2,6-DAT in the presence of S9 activation. The mutagenicity of 2,6-DAT was similar to that of 2,4-DAT in the presence of S9 activation (in strain TA98, 1036 vs. 1316 His^+ revertants per plate at 625 μg of 2,4-DAT and 2,6-DAT, respectively; in strain YG1024, 3460 vs. 3896 His^+ revertants per plate at 156 μg of 2,4-DAT and 2,6-DAT, respectively).

TABLE 1
Quantification of Hepatocyte Proliferation

	No. of Rats	No. of Total Nuclei	No. of Ki-67–Positive Nuclei	Index
Basal diet	5	2170.8 ± 890.9	27.4 ± 8.1	0.013 ± 0.004
Basal diet (DEN)	5	1749.6 ± 729.2[a]	73.8 ± 19.7	0.042 ± 0.009*
125 ppm 2,4-DAT	5	1700.2 ± 700.1[a]	14.0 ± 6.6	0.008 ± 0.005
250 ppm 2,4-DAT	5	1436.4 ± 596.7[a]	44.4 ± 10.5	0.031 ± 0.007*
500 ppm 2,4-DAT	5	1308.6 ± 537.6[a]	20.4 ± 9.0	0.015 ± 0.006
500 ppm 2,6-DAT	5	2048.8 ± 860.8	17.8 ± 7.4	0.014 ± 0.004

[a]Total number of nuclei was significantly decreased compared to the basal diet treatment group.
*Significantly different from the basal diet group ($p < 0.01$).

These results suggest that both DATs are mutagenic in the presence of S9 activation *in vitro* and also that *O*-acetylation is important for the metabolic activation.

In Vivo Mutagenicity of 2,4-DAT

For the initial *in vivo* genotoxicity assay, we examined MN formation in the peripheral blood of F344 *gpt* delta rats treated with 2,4-DAT or 2,6-DAT. However, no significant increase in MN frequency was observed in any of the treated groups (Supplementary table 4).

Next, we examined the mutagenicity of the DATs in the livers and kidneys of the rats. *gpt* MFs were significantly increased in the livers of 2,4-DAT–treated rats at all three doses and in the DEN-positive control, compared to the control group (Fig. 3, Supplementary table 3). No increases in MFs were observed in the livers of 2,6-DAT–treated rats or in the kidneys of either 2,4-DAT– or 2,6-DAT–treated rats. To characterize the *gpt* mutations in the liver, we performed DNA sequencing (Table 3). The predominant base substitutions were G:C-to-A:T transitions and G:C-to-T:A and G:C-to-C:G transversions in the 2,4-DAT–treated groups. In addition, base substitutions at A:T bps were also induced. In the DEN-treated positive control group, A:T-to-T:A transversions were the most predominant type of mutation. Spi$^-$ MFs in the liver were also significantly increased in 2,4-DAT treatment groups at doses of 250 and 500 ppm and in the DEN-treated group (Table 4). They were not increased by treatment with 2,6-DAT. DNA sequence analysis revealed that the specific mutant frequency (SMF) of a −1 frameshift at run sequences such as GGGG in the *gam* gene was increased more than fourfold after treatment with 500 ppm 2,4-DAT, while the SMF of deletions of more than two bps was not enhanced at this dose (Supplementary table 5). Thus, most of the Spi$^-$ mutations were −1 frameshift mutations at run sequences, and large deletion mutations were not significantly induced by treatment with 2,4-DAT.

TABLE 2
Quantification of GST-P–Positive Foci

	No. of Rats	No. of Foci (No./cm^2)	Area of Foci (mm^2/cm^2)
Basal diet	5	0.00 ± 0.00	0.000 ± 0.000
Basal diet (DEN)	5	78.92 ± 17.70**	1.924 ± 0.655**
125 ppm 2,4-DAT	5	0.00 ± 0.00	0.000 ± 0.000
250 ppm 2,4-DAT	5	1.19 ± 1.21	0.022 ± 0.023
500 ppm 2,4-DAT	5	6.05 ± 3.93*	0.502 ± 0.476*
500 ppm 2,6-DAT	5	0.00 ± 0.00	0.000 ± 0.000

*Significantly different from the basal diet group ($p < 0.05$).
**Significantly different from the basal diet group ($p < 0.01$).

DISCUSSION

In the regulatory sciences, a default assumption is that genotoxic carcinogens have no thresholds for their activities, and thus, no acceptable daily intake can be set for these chemicals when they are used as food additives, pesticides, or veterinary medicines (Kirsch-Volders *et al.*, 2000; Nohmi, 2008). It is thought that single molecules of genotoxic compounds can induce mutations, and thus, genotoxic carcinogens impose carcinogenic risks to humans even at very low doses. However, how the genotoxicity of chemicals should be defined is not entirely clear. Currently, more than 200 genotoxicity assays have been proposed (Preston and Hoffmann, 2007). Unsurprisingly, the results among the various genotoxicity assays are inconsistent. The aromatic amine structural isomers 2,4-DAT and 2,6-DAT are an interesting reference pair that illustrates the inconsistency between *in vitro* and *in vivo* results (Cunningham *et al.*, 1989). Both 2,4-DAT and 2,6-DAT are mutagenic *in vitro* in *S. typhimurium* strains, but only 2,4-DAT is carcinogenic in mice and rats (NTP, 1979).

In this study, we confirmed *in vitro* genotoxicity with *S. typhimurium* TA98 and YG1024 and explored *in vivo* genotoxicity with F344 *gpt* delta rats. Both DATs were mutagenic in the *S. typhimurium* strains *in vitro* when the S9 activation system was present (Fig. 2). In contrast, only 2,4-DAT was mutagenic in the livers of rats (Fig. 3, Table 4, Supplementary table 4). Both *gpt* and Spi$^-$ MFs in the liver were significantly increased in 2,4-DAT–treated rats compared to those in the control group. We did not observe any increase in *gpt* MFs in the livers of 2,6-DAT–treated rats or in the kidneys of 2,4- or 2,6-DAT–treated rats (Fig. 3, Supplementary table 4). Kidney may not have capacity to activate 2,4-DAT as in the case of bone marrow (see below). We identified preneoplastic lesions (i.e., GST-P–positive foci) in the livers of rats treated with 250 and 500 ppm 2,4-DAT (Table 2) but not in the livers of rats treated with 2,6-DAT. Generally, proliferation is activated in cancer cells. Ki-67 is a nuclear marker of cell proliferation and detectable in cells at all phases of the cell cycles except G_0 (Gerdes *et al.*, 1983). The Ki-67

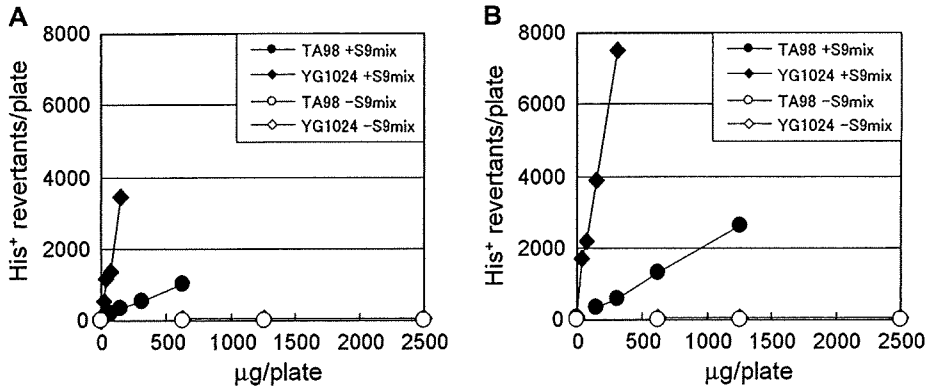

FIG. 2. Mutagenic activity of 2,4-DAT (A) and 2,6-DAT (B) in *Salmonella typhimurium* strains TA98 (circle) and YG1024 (rhombus). Filled circle and rhombus assayed with S9 mix; open circle and rhombus assayed without S9 mix.

labeling index is a measure of tumor proliferation and reported the association with liver and breast cancer outcome (de Azambuja *et al.*, 2007; Nolte *et al.*, 1998). The increase in Ki-67 index suggested the precancerous status of liver of rats treated by 2,4-DAT (Table 1, Fig. 1). We conclude from these results that genotoxicity assays (i.e., *gpt* and Spi$^-$ assays) and short-term carcinogenicity assays (i.e., GST-P–positive foci formation) can be conducted with F344 *gpt* delta rats. Because we observed genotoxicity in the target organ of carcinogenicity, these results strongly suggest that the carcinogenicity of 2,4-DAT is due to genotoxic activities. Integration of the genotoxicity assay with the pathological assay including GST-P–positive foci formation in *gpt* delta rats could reduce the number of animals necessary for these assays; this would contribute to the adoption of the 3R (reduction, replacement, and refinement) principle for animal use in the life sciences (Balls, 1997). It should be mentioned, however, that GST-P–positive foci formation often needs long treatment periods, for example, 16 and 24 weeks, respectively, for 2-amino-3,8-dimethylimidazo[4,5-*f*]-quinoxaline and 2-acetylaminofluorene (Bagnyukova *et al.*, 2008; Tsuda *et al.*, 2003) and such long treatments may increase the risk of false-positive results of mutations due to nongenotoxic mechanisms caused by chronic toxicity, for example, tumor induction and inflammatory responses (Thybaud et al., 2003).

Why do both 2,6-DAT and 2,4-DAT exhibit mutagenicity *in vitro*? The inconsistency between *in vitro* and *in vivo* results could be due to the different metabolic pathways of 2,6-DAT *in vitro* and *in vivo*. It is plausible that a DAT amino group is first oxidized by a specific cytochrome P450 (e.g., CYP1A2), and the resulting *N*-hydroxy group is further activated by OAT, which leads to the generation of nitrenium ions that can bind to DNA *in vitro* (Watanabe *et al.*, 1994). *In vitro,* both DATs were mutagenic only in the presence of S9 activation, and strain YG1024, which overexpresses OAT, exhibited greater sensitivity to the DATs than did strain TA98 (Fig. 2). Both *S. typhimurium* strains possess GC repetitive sequences in the *hisD* gene that serve as target sites for mutations. We speculate, therefore, that 2,4-DAT could be activated *in vivo* via the pathway described above and induce mostly guanine adducts in DNA. In fact, it was reported that 2,4-DAT induces DNA

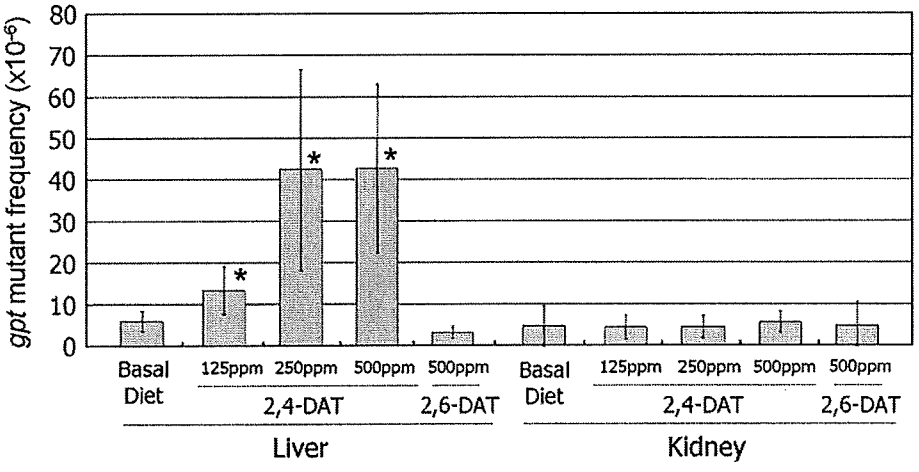

FIG. 3. MFs of *gpt* genes. Values represent mean SD ($n = 5$). Significant differences were observed in 2,4-DAT–treated livers compared to livers from rats fed negative control basal diet. *$p < 0.05$.

TABLE 3
Classification of *gpt* Mutations in *gpt* Delta Rat Livers

Type of gpt Mutation	Basal Diet		125 ppm 2,4-DAT		250 ppm 2,4-DAT		500 ppm 2,4-DAT		500 ppm 2,6-DAT		Basal Diet (DEN)	
	No.	%	No.	%	No.	%	No.	%	No.	%	No.	%
Base substitution												
Transition												
G:C → A:T	4	22	15	26	18	38	12	35	4	27	13	22
(CpG)	(1)		(6)		(6)		(3)		(1)		(3)	
A:T → G:C	1	6	1	2	5	11	1	3	3	20	12	21
Transversion												
G:C → T:A	4	22	16	28	12	26	6	18	4	27	3	5
G:C → C:G	1	6	7	12	4	9	7	21	0	0	0	0
A:T → T:A	0	0	5	9	4	9	1	3	1	7	23	40
A:T → C:G	1	6	4	7	3	6	1	3	0	0	7	12
Deletion												
−1	4	22	3	5	1	2	2	6	1	7	0	0
>2	2	11	2	3	0	0	1	3	2	13	0	0
Insertion	1	6	3	5	0	0	1	3	0	0	0	0
Others	0	0	2	3	0	0	2	6	0	0	0	0
Total	18	100	58	100	47	100	34	100	15	100	58	100

adducts in the livers of rats over 6000 times more efficiently than does 2,6-DAT (Taningher *et al.*, 1995). The sequence analysis that we conducted indicates that most of the mutations induced by 2,4-DAT at 500 ppm were guanine base substitutions; that is, G:C-to-A:T, G:C-to-T:A, and G:C-to-C:G (Table 3). 2,6-DAT might be more efficiently detoxicated than 2,4-DAT *in vivo* because its *para* site at position 4 can be oxidized and subsequently conjugated by phase II enzymes (Cunningham *et al.*, 1989). Detoxication of 2,6-DAT by phase II enzymes may be ineffective *in vitro* compared to *in vivo*. Appropriate cofactors, for example, uridine 5′-diphosphoric acid P2-β-D-glucopyranuronosyl ester for glucuronidation, may be needed to effectively detoxify the active metabolites of 2,6-DAT *in vitro*. At present, however, we cannot rule out the possibility that other factors, such as DNA repair, cell proliferation, translesion DNA synthesis, or apoptosis, might be involved in the differences in mutagenicity of 2,6-DAT *in vitro* and *in vivo*.

TABLE 4
Spi$^-$ Mutant Frequency in Rat Livers

Treatment	No. of Rats	Mutant Frequency ($\times 10^{-6}$) (Mean ± SD)	*p* Value (*t*-test)
Basal diet	5	4.43 ± 1.99	
Basal diet (DEN)	5	341.22 ± 180.91	0.002
125 ppm 2,4-DAT	5	8.20 ± 4.75	0.07
250 ppm 2,4-DAT	5	13.42 ± 4.83	0.003
500 ppm 2,4-DAT	5	15.98 ± 4.45	0.0004
500 ppm 2,6-DAT	5	5.49 ± 2.53	0.241

In addition to the discrepancy between *in vitro* and *in vivo* mutagenicity, neither 2,4-DAT nor 2,6-DAT was genotoxic in the bone marrows of rats according to the MN assay (Supplementary table 3). 2,4-DAT is also not mutagenic when applied to MutaMouse skin (Kirkland and Beevers, 2006). Thus, we suggest that the negative results of the MN assay may be due to inefficient metabolic activation of 2,4-DAT at extrahepatic sites. Alternatively, the active metabolites generated in the liver may not reach the bone marrow. The poor metabolic activation in extrahepatic sites and/or short half-lives of the active metabolites may also account for the negative results of the MN assay with DEN in the bone marrow (Supplementary table 3). The MN assay is usually the first choice for *in vivo* genotoxicity assays in the development of pharmaceuticals; our results indicate that rather than relying on the MN assay in the bone marrow, genotoxicity should be evaluated in multiple organs, including the target organs of carcinogenicity.

The Spi$^-$ assay is unique to *gpt* delta mice and rats and identifies deletion-type mutations (Nohmi *et al.*, 2000). Previous studies with *gpt* delta mice suggested that genotoxic compounds and physical factors (e.g., radiation) induce different types of deletion mutations *in vivo* (Nohmi and Masumura, 2005). For example, heavy-ion radiation, ultraviolet B radiation, and mitomycin C induce large deletions in the liver, epidermis, and bone marrow, respectively, at molecular sizes of >1 kbp (Horiguchi *et al.*, 2001; Masumura *et al.*, 2002; Takeiri *et al.*, 2003). In contrast, aromatic amines such as 2-amino-1-methyl-6-phenylimidazo[4,5-b]pyridine (PhIP) and aminophenylnorharman (APNH) induce −1 frameshift mutations in runs of guanine bases in the colon and liver, respectively (Masumura *et al.*, 2000, 2003). We characterized Spi$^-$ mutants obtained from the livers of rats treated with 500-ppm 2,4-DAT and concluded that, like PhIP and APNH, 2,4-DAT induces mostly −1 frameshift mutations (Supplementary table 5). These results suggest that Spi$^-$ assay, as well as the *gpt* assay, is useful for characterizing mutations, which may constitute the molecular basis of chemically induced carcinogenesis.

At the 2006 International Conference on Harmonization of Technical Requirements for Registration of Pharmaceuticals for Human Use meeting held in Yokohama, Japan, revisions of the guidelines for a basic test battery of *in vitro* and *in vivo* genotoxicity tests were discussed (Hayashi, 2008). The current guidelines recommend two *in vitro* assays (Ames test and either a mammalian chromosome aberration test or a mammalian gene mutation test) plus one *in vivo* assay (usually MN test). Because of the high rate of false positives with *in vitro* mammalian cell assays (Kirkland *et al.*, 2005), however, an alternative test battery was proposed at the meeting (Hayashi, 2008). The new battery is composed of one *in vitro* assay (Ames test) plus two *in vivo* assays (MN test plus a second *in vivo* test such as a transgenic assay or *in vivo* comet assay). It is possible to choose the classical battery of two *in vitro* assays plus one

in vivo assay instead of the alternative new battery. With the 3R principle in mind, integration of *in vivo* genotoxicity assays and a 28-day repeated dose toxicity assay was also discussed. *In vivo* mutagenicity assays and an *in vivo* MN assay can be integrated into a 28-day repeated dose toxicity study when transgenic rodents are used (Thybaud *et al.*, 2003). In this study, we found that an *in vivo* genotoxicity assay and a short-term bioassay for liver carcinogenesis using GST-P–positive foci as an end point of preneoplastic lesions can be conducted with F344 *gpt* delta rats. Integration of the two assays using transgenic rats may further facilitate adoption of the 3R principle in regulatory toxicology.

SUPPLEMENTARY DATA

Supplementary data are available online at http://toxsci.oxfordjournals.org/.

FUNDING

Ministry of Education, Culture, Sports, Science and Technology, Japan (18201010); the Ministry of Health, Labour and Welfare, Japan (MHLW; H21-Food-General-009); the Japan Health Science Foundation (KHB1007); MHLW (20 designated-8).

REFERENCES

Aoki, Y., Hashimoto, A. H., Amanuma, K., Matsumoto, M., Hiyoshi, K., Takano, H., Masumura, K., Itoh, K., Nohmi, T., and Yamamoto, M. (2007). Enhanced spontaneous and benzo(a)pyrene-induced mutations in the lung of *Nrf2*-deficient *gpt* delta mice. *Cancer Res.* **67,** 5643–5648.

Bagnyukova, T. V., Tryndyak, V. P., Montgomery, B., Churchwell, M. I., Karpf, A. R., James, S. R., Muskhelishveli, L., Beland, F. A., and Pogribny, I. P. (2008). Genetic and epigenetic changes in rat preneoplastic liver tissue induced by 2-acetylaminofluorene. *Carcinogenesis* **29,** 638–646.

Balls, M. (1997). The three Rs concept of alternatives to animal experimentation. In *Animal Alternatives* (L. F. M. van Zutphen and M. Balls, Eds.), pp. 27–41. Elsevier, Amsterdam.

Cunningham, M. L., Burka, L. T., and Matthews, H. B. (1989). Metabolism, disposition, and mutagenicity of 2,6-diaminotoluene, a mutagenic non-carcinogen. *Drug Metab. Dispos.* **17,** 612–617.

Cunningham, M. L., Hayward, J. J., Shane, B. S., and Tindall, K. R. (1996). Distinction of mutagenic carcinogens from a mutagenic noncarcinogen in the big blue transgenic mouse. *Environ. Health Perspect.* **104**(Suppl. 3), 683–686.

de Azambuja, E., Cardoso, F., de Castro, G., Jr, Colozza, M., Mano, M. S., Durbecq, V., Sotiriou, C., Larsimont, D., Piccart-Gebhart, M. J., and Paesmans, M. (2007). Ki-67 as prognostic marker in early breast caner: a meta-analysis of published studies involving 12,155 patients. *Br. J. Cancer.* **96,** 1504–1513.

Eastmond, D. A., Hartwig, A., Anderson, D., Anwar, W. A., Cimino, M. C., Dobrev, I., Douglas, G. R., Nohmi, T., Phillips, D. H., and Vickers, C. (2009). Mutagenicity testing for chemical risk assessment: update of the WHO/IPCS Harmonized Scheme. *Mutagenesis* **24,** 341–349.

Gerdes, J., Schwab, U., Lemke, H., and Stein, H. (1983). Production of a mouse monoclonal antibody reactive with a human nuclear antigen associated with cell proliferation. *Int. J. Cancer* **31,** 13–20.

Hashimoto, A. H., Amanuma, K., Masumura, K., Nohmi, T., and Aoki, Y. (2009). *In vivo* mutagenesis caused by diesel exhaust in the testis of *gpt* delta mouse. *Genes Environ.* **31,** 1–8.

Hayashi, H., Kondo, H., Masumura, K., Shindo, Y., and Nohmi, T. (2003). Novel transgenic rat for in vivo genotoxicity assays using 6-thioguanine and Spi⁻selection. *Environ. Mol. Mutagen.* **41,** 253–259.

Hayashi, M. (2008). Update on the maintenance of the ICH S2 genetic toxicology. *Pharm. Regul. Sci.* **39,** 515–521.

Heddle, J. A., Dean, S., Nohmi, T., Boerrigter, M., Casciano, D., Douglas, G. R., Glickman, B. W., Gorelick, N. J., Mirsalis, J. C., Martus, H. J., *et al.* (2000). *In vivo* transgenic mutation assays. *Environ. Mol. Mutagen.* **35,** 253–259.

Horiguchi, M., Masumura, K. I., Ikehata, H., Ono, T., Kanke, Y., and Nohmi, T. (2001). Molecular nature of ultraviolet B light-induced deletions in the murine epidermis. *Cancer Res.* **61,** 3913–3918.

Ito, N., Imaida, K., Asamoto, M., and Shirai, T. (2000). Early detection of carcinogenic substances and modifiers in rats. *Mutat. Res.* **462,** 209–217.

Kirkland, D., Aardema, M., Henderson, L., and Muller, L. (2005). Evaluation of the ability of a battery of three *in vitro* genotoxicity tests to discriminate rodent carcinogens and non-carcinogens I. Sensitivity, specificity and relative predictivity. *Mutat. Res.* **584,** 1–256.

Kirkland, D., and Beevers, C. (2006). Induction of *LacZ* mutations in Muta Mouse can distinguish carcinogenic from non-carcinogenic analogues of diaminotoluenes and nitronaphthalenes. *Mutat. Res.* **608,** 88–96.

Kirsch-Volders, M., Aardema, M., and Elhajouji, A. (2000). Concepts of threshold in mutagenesis and carcinogenesis. *Mutat. Res.* **464,** 3–11.

Maron, D. M., and Ames, B. N. (1983). Revised methods for the salmonella mutagenicity test. *Mutat. Res.* **113,** 173–215.

Masumura, K., Matsui, M., Katoh, M., Horiya, N., Ueda, O., Tanabe, H., Yamada, M., Suzuki, H., Sofuni, T., and Nohmi, T. (1999). Spectra of *gpt* mutations in ethylnitrosourea-treated and untreated transgenic mice. *Environ. Mol. Mutagen.* **34,** 1–8.

Masumura, K., Matsui, K., Yamada, M., Horiguchi, M., Ishida, K., Watanabe, M., Wakabayashi, K., and Nohmi, T. (2000). Characterization of mutations induced by 2-amino-1-methyl-6-phenylimidazo[4,5-*b*]pyridine in the colon of *gpt* delta transgenic mouse: novel G: C deletions beside runs of identical bases. *Carcinogenesis* **21,** 2049–2056.

Masumura, K., Kuniya, K., Kurobe, T., Fukuoka, M., Yatagai, F., and Nohmi, T. (2002). Heavy-ion-induced mutations in the *gpt* delta transgenic mouse: comparison of mutation spectra induced by heavy-ion, X-ray, and gamma-ray radiation. *Environ. Mol. Mutagen.* **40,** 207–215.

Masumura, K., Totsuka, Y., Wakabayashi, K., and Nohmi, T. (2003). Potent genotoxicity of aminophenylnorharman, formed from non-mutagenic norharman and aniline, in the liver of *gpt* delta transgenic mouse. *Carcinogenesis* **24,** 1985–1993.

National Toxicology Program. (1979). Bioassay of 2,4-diaminotoluene for possible carcinogenicity. *Natl. Cancer Inst. Carcinog. Tech. Rep. Ser.* **162,** 1–139.

National Toxicology Program. (1980). Bioassay of 2,6-toluenediamine dihydrochloride for possible carcinogenicity (CAS No. 15481-70-6). *Natl. Toxicol. Program Tech. Rep. Ser.* **200,** 1–123.

Nohmi, T. (2008). Possible mechanisms of practical thresholds for genotoxicity. *Genes Environ.* **30,** 108–113.

Nohmi, T., Katoh, M., Suzuki, H., Matsui, M., Yamada, M., Watanabe, M., Suzuki, M., Horiya, N., Ueda, O., Shibuya, T., *et al.* (1996). A new

transgenic mouse mutagenesis test system using Spi⁻and 6-thioguanine selections. *Environ. Mol. Mutagen.* **28,** 465–470.

Nohmi, T., and Masumura, K. (2005). Molecular nature of intrachromosomal deletions and base substitutions induced by environmental mutagens. *Environ. Mol. Mutagen.* **45,** 150–161.

Nohmi, T., Suzuki, T., and Masumura, K. (2000). Recent advances in the protocols of transgenic mouse mutation assays. *Mutat. Res.* **455,** 191–215.

Nolte, M., Werner, M., Nasarek, A., Bektas, H., von Wasielewski, R., Klempnauer, J., and Georgii, A. (1998). Expression of proliferation associated antigens and detection of numerical chromosome aberrations in primary human liver tumors: relevance to tumor characteristic and prognosis. *J. Clin. Pathol.* **51,** 47–51.

Ogiso, T., Tatematsu, M., Tamano, S., Tsuda, H., and Ito, N. (1985). Comparative effects of carcinogens on the induction of placental glutathione S-transferase-positive liver nodules in a short-term assay and of hepatocellular carcinomas in a long-term assay. *Toxicol. Pathol.* **13,** 257–265.

Preston, R. J., and Hoffmann, G. R. (2007). Genetic toxicology. In *Casarett and Doull's Toxicology: The Basic Science of Poisons* (C. D. Klaassen, Ed.), pp. 381–413. The McGraw-Hill Companies, Inc., New York.

Shibata, A., Maeda, D., Ogino, H., Tsutsumi, M., Nohmi, T., Nakagama, H., Sugimura, T., Teraoka, H., and Masutani, M. (2009). Role of Parp-1 in suppressing spontaneous deletion mutation in the liver and brain of mice at adolescence and advanced age. *Mutat. Res.* **664,** 20–27.

Takeiri, A., Mishima, M., Tanaka, K., Shioda, A., Ueda, O., Suzuki, H., Inoue, M., Masumura, K., and Nohmi, T. (2003). Molecular characterization of mitomycin C-induced large deletions and tandem-base substitutions in the bone marrow of *gpt* delta transgenic mice. *Chem. Res. Toxicol.* **16,** 171–179.

Taningher, M., Peluso, M., Parodi, S., Ledda-Columbano, G. M., and Columbano, A. (1995). Genotoxic and non-genotoxic activities of 2,4- and 2,6-diaminotoluene, as evaluated in Fischer-344 rat liver. *Toxicology* **99,** 1–10.

Thybaud, V., Dean, S., Nohmi, T., de Boer, J., Douglas, G. R., Glickman, B. W., Gorelick, N. J., Heddle, J. A., Heflich, R. H., Lambert, I., *et al.* (2003). *In vivo* transgenic mutation assays. *Mutat. Res.* **540,** 141–151.

Tsuda, H., Fukushima, S., Wanibuchi, H., Morimura, K., Nakae, D., Imaida, K., Tatematsu, M., Hirose, M., Wakabayashi, K., and Moore, M. A. (2003). Value of GST-P positive preneoplastic hepatic foci in dose-response studies of hepatocarcinogenesis: evidence for practical thresholds with both genotoxic and nongenotoxic carcinogens. A review of recent work. *Toxicol. Pathol.* **31,** 80–86.

Umemura, T., Kanki, K., Kuroiwa, Y., Ishii, Y., Okano, K., Nohmi, T., Nishikawa, A., and Hirose, M. (2006). *In vivo* mutagenicity and initiation following oxidative DNA lesion in the kidneys of rats given potassium bromate. *Cancer Sci.* **97,** 829–835.

Umemura, T., Tasaki, M., Kijima, A., Okamura, T., Inoue, T., Ishii, Y., Suzuki, Y., Masui, N., Nohmi, T., and Nishikawa, A. (2009). Possible participation of oxidative stress in causation of cell proliferation and *in vivo* mutagenicity in kidneys of *gpt* delta rats treated with potassium bromate. *Toxicology* **257,** 46–52.

Watanabe, M., Igarashi, T., Kaminuma, T., Sofuni, T., and Nohmi, T. (1994). N-hydroxyarylamine *O*-acetyltransferase of Salmonella typhimurium: proposal for a common catalytic mechanism of arylamine acetyltransferase enzymes. *Environ. Health Perspect.* **102**(Suppl. 6), 83–89.

Xu, A., Smilenov, L. B., He, P., Masumura, K., Nohmi, T., Yu, Z., and Hei, T. K. (2007). New insight into intrachromosomal deletions induced by chrysotile in the *gpt* delta transgenic mutation assay. *Environ. Health Perspect.* **115,** 87–92.

RADIATION RESEARCH 173, 138–147 (2010)
0033-7587/10 $15.00

DOI: 10.1667/RR1932.1

Radiation Dose-Rate Effect on Mutation Induction in Spleen and Liver of *gpt* delta Mice

Naohito Okudaira,[a] Yoshihiko Uehara,[a] Kazuo Fujikawa,[b] Nao Kagawa,[b] Akira Ootsuyama,[c] Toshiyuki Norimura,[c] Ken-ichi Saeki,[d] Takehiko Nohmi,[e] Ken-ichi Masumura,[e] Tsuneya Matsumoto,[f] Yoichi Oghiso,[f] Kimio Tanaka,[f] Kazuaki Ichinohe,[f] Shingo Nakamura,[f] Satoshi Tanaka[f] and Tetsuya Ono[a,1]

[a] *Department of Cell Biology, Graduate School of Medicine, Tohoku University, Sendai 980-8575, Japan;* [b] *Deparment of Life Science, Faculty of Science and Technology, Kinki University, Kowakae, Higashiosaka 577-8502, Japan;* [c] *Department of Radiation Biology and Health, University of Occupational and Environmental Health, Kitakyushu, 807-8555, Japan;* [d] *Yokohama College of Pharmacy, Totsuka-ku, Yokohama 245-0066, Japan;* [e] *Division of Genetics and Mutagenesis, National Institute of Health Sciences, Kamiyoga, Setagaya-ku, Tokyo 158-8501, Japan; and* [f] *Institute for Environmental Sciences, Rokkasho, Aomori 039-3212, Japan*

Okudaira, N., Uehara, Y., Fujikawa, K., Kagawa, N., Ootsuyama, A., Norimura, T., Saeki, K., Nohmi, T., Masumura, K., Matsumoto, T., Oghiso, Y., Tanaka, K., Ichinohe, K., Nakamura, S., Tanaka, S. and Ono, T. Radiation Dose-Rate Effect on Mutation Induction in Spleen and Liver of *gpt* delta Mice. *Radiat. Res.* 173, 138–147 (2010).

The effect of dose rate on radiation-induced mutations in two somatic tissues, the spleen and liver, was examined in transgenic *gpt* delta mice. These mice can be used for the detection of deletion-type mutations, and these are the major type of mutation induced by radiation. The dose rates examined were 920 mGy/min, 1 mGy/min and 12.5 μGy/min. In both tissues, the number of mutations increased with increasing dose at each of the three dose rates examined. The mutation induction rate was dependent on the dose rate. The mutation induction rate was higher in the spleen than in the liver at the medium dose rate but was similar in the two tissues at the high and low dose rates. The mutation induction rate in the liver did not show much change between the medium and low dose rates. Analysis of the molecular nature of the mutations indicated that 2- to 1,000-bp deletion mutations were specifically induced by radiation in both tissues after high- and low-dose-rate irradiation. The occurrence of deletion mutation without any sequence homology at the break point was elevated in spleen after high-dose-rate irradiation. The results indicate that the mutagenic effects of radiation in somatic tissues are dependent on dose rate and that there is some variability between tissues.

INTRODUCTION

Most radiation effects in biological systems influenced by the dose rate. Quantitative studies of the dose-rate effect are important for risk estimation as well as for understanding the mechanisms involved in radiation effects. Mutations are one of the most extensively studied biological end points, because they could be involved in long-term effects of radiation such as cancer induction, life-shortening and transgenerational effects. However, most studies have been performed using cultured cells, and studies in animal tissues have been limited to spleen lymphocytes (*1*), intestinal stem cells (*2*) and germ-line cells in gonads (*3, 4*). Mutations in germ-line cells were studied extensively by two groups working with mice (*3, 4*). They found that the efficiency of mutation induction was reduced to one-third as the dose rate decreased from 900 mGy/min to 8 mGy/min. Below 8 mGy/min, Russell *et al.* did not find any significant variation in mutation induction efficiency for dose rates down to 7 μGy/min (*4*). Lyon *et al.*, on the other hand, suggested that the efficiency of mutation induction might be elevated at 10 μGy/min compared to the dose-rate range of 50 μGy/min to 8 mGy/min, although the difference was small (*3*). A dose-rate effect in germ cells was also observed in the fish *Oryzias latipes* (*5*). Studies in somatic tissues have been performed using mice. One study involved mutations in the *Hprt* gene in splenic lymphocytes (*1*), and another study was of mutations in the *Dlb1* gene in the stem cells of the small intestine (*2*). Dose-rate effects were found in these cells, with differences between high (about 1 Gy/min) and low dose rates (0.099 mGy/min for *Hprt* and 10 mGy/min for *Dlb1*). In the *Hprt* gene in splenic lymphocytes, the efficiency of mutation induction was similar between 690 μGy/min and 99 μGy/min. Chromosomal translocations in blood lymphocytes were also reported to show similar radiosensitivities at 3.5, 14 and 28 μGy/min (*6*). Somatic cells in culture also revealed a similar dose-rate dependence [(*7, 8*) and references therein]. All of these studies found good agreement on the overall pattern of

[1] Address for correspondence: Department of Cell Biology, Graduate School of Medicine, Tohoku University, Seiryo-machi 2-1, Aoba-ku, Sendai 980-8575, Japan; e-mail: tono@mail.tains.tohoku.ac.jp.

observed dose-rate dependences: a high efficiency of mutation induction at dose rates of 0.5–2 Gy/min and low efficiencies in a dose-rate range of 3.5 μGy/min to 50 mGy/min.

To examine dose-rate effects in very low-dose-rate ranges, Valenchic and Knudson suggested that mutation induction as well as many other biological end points might be elevated in certain low-dose-rate ranges, which would make the dose-rate–response curves appear parabolic (*9, 10*). On the other hand, more recent studies on chromosomal abnormalities in splenic lymphocytes revealed a constant decline of efficiency in the dose-rate range of 890 mGy/min to 0.76 μGy/min (*11*). Thus more detailed studies on dose-rate effects are desirable, especially in different somatic tissues. The purpose of the present study was to elucidate the dose-rate effects of radiation-induced mutation in two somatic tissues, the spleen and liver.

The main problem for mutation studies in somatic tissues *in vivo* was the lack of a method to detect mutations. However, this has been overcome by the creation of transgenic mice that are suitable for mutation assays. These mice contain bacterial genes in their genome, and the bacterial genes can be assayed for mutations by using bacterial systems (*12*). In the work described here, transgenic *gpt* delta mice were used to study dose-rate effects in the spleen and liver. These mice contain lambda EG10 genomic DNA in chromosome 17, and the Spi^- assay can be applied to focus exclusively on deletion-type mutations in the *red-gam* genes located in the central part of the lambda EG10 genome (*13, 14*). In previous studies, deletions were found to be the predominant type of mutation induced by radiation in the spleen and liver when a 3.1-kbp-long *lacZ* gene was used to monitor mutations (*15, 16*). Nohmi *et al.* (*17*) and Furuno-Fukushi *et al.* (*18*) reported that the *gpt* delta mice can be used to detect mutations induced by 5 to 50 Gy of radiation.

MATERIALS AND METHODS

Mice and Irradiation

Transgenic *gpt* delta mice containing lambda EG10 genomic DNA (*15*) were mated to SWR mice that contained the *Dlb1*^{b} allele (*19*), and F_1 mice were used to compare mutations in the *red-gam* gene and the *Dlb1* gene. The results of a study on the *Dlb1* gene will be reported separately. Some F_1 mice were irradiated with ^{137}Cs γ rays at dose rates of 920 mGy/min or 1 mGy/min at 2 months of age in the University of Occupational and Environmental Health and were killed humanely 1 week after the end of the irradiation. Spleen and liver were excised, frozen on dry ice and kept at –70°C until use. Other F_1 mice were irradiated with a very low dose rate of 12.5 μGy/min for 483 consecutive days using a low-dose-rate irradiation facility at the Institute for Environmental Sciences. The exposures were started at 2 months of age, and the mice were exposed for 22 h every day. The remaining 2 h (10:00 am to 12:00 noon) were spent checking the health of the mice, changing food, water and cages, and cleaning the room. Control mice were treated in the same way without irradiation in a neighboring room. The mice were sampled 1 week after the end of irradiation. Spleens and livers were excised, frozen on dry ice, and kept at –70°C until use. All mice were kept under SPF conditions (*20, 21*). All procedures were conducted under the Guidelines for Animal Experiments of the University of Occupational and Environmental Health and the Institute for Environmental Sciences.

TABLE 1
Common Alterations Found in *gpt* delta Mice

Location	Alteration[a]
19,377	TTACC → TTGCC
19,787	CCGC → CC(T)GC (+1)
20,705	CTGCT → CTACT
23,118	GTTTC → GTCTC
23,849	GTGAA → GTAAA
24,068	TCATC → TCTTC
34,896	CACC → CA(A)CC (+1)
35,010	CAGAC → CAAAC
38,668	CAGTG → CAATG
39,732	GGAAA → GGGAA

[a] Base substitutions are underlined and the inserted bases are shown in parentheses. +1 indicates one base insertion.

Mutation Assays

Genomic DNA was extracted from spleens and livers using phenol. Lambda EG10 DNA integrated in the mouse genome was retrieved in the form of a phage by mixing the genomic DNA with a packaging extract (Transpack® Packaging Extract, Stratagene, La Jolla, CA) according to the manufacturer's instructions. The recovered phage was assayed by plaque formation using *E. coli* XL-1 Blue MRA. The phages containing mutations in the *red-gam* genes in the lambda phage were detected as plaques on P2-lysogenic E. coli XL-1 Blue MRA (P2) as described previously (*13, 14*).

DNA Sequence Analysis

Nucleotide sequences of the mutant phage DNA were determined with PCR amplification and sequencing of the amplified fragments. First, the 1.8-kbp *red-gam* gene was amplified with PCR. When the PCR product was obtained, it was sequenced from both ends of the fragment. When a PCR product was not produced, it was assumed that one of the PCR primer sites was deleted, and extended PCR amplification to the flanking regions using different primers was performed. The primers were chosen from nearby adjacent locations, and appropriate primers were sought by continuously testing primers sequentially from nearby locations. When PCR successfully produced a DNA fragment, it was sequenced to determine the end of the deletion mutation. The primers and their locations have been described previously (*14*). The sequences obtained were compared to those in wild-type lambda EG10.

From the sequence analyses, alterations in 10 locations in and around the *red-gam* gene were found. Since these 10 alterations were common in more than four wild-type lambda EG10 phage isolated from the mice, it was concluded that these alterations were inherent in the lambda EG10 sequence in the *gpt* delta mice used. They are listed in Table 1. All of the other alterations found were unique to mutant phage and were not found in at least three wild-type clones. They were counted as mutations. When unusual mutations were found, such as tandem, multiple or complex mutations, the alterations were confirmed by sequencing both the upper and lower DNA strands.

In one mutant clone, there was an insertion of a part of the lambda EG10 sequence in the *red-gam* gene. To determine whether the inserted sequence was produced by duplication of the original sequence or by translocation of DNA fragment, the presence of the original sequence was examined by PCR amplification using the

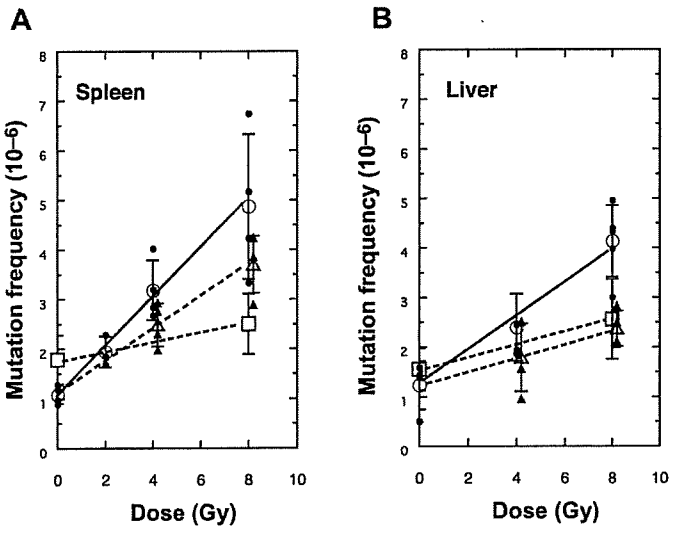

FIG. 1. Radiation-induced mutations at different dose rates. *Gpt* delta × SWR F_1 mice were irradiated with γ rays at a rate of 920 mGy/min, 1 mGy/min and 12.5 μGy/min. Mutation frequencies in the spleen (panel A) and liver (panel B) were determined in the *red-gam* genes. The small closed symbols indicate mutant frequencies for each mouse and the large open symbols indicate the means ± SD. Circles with solid lines indicate the dose response at 920 mGy/min, triangles with dotted lines 1 mGy/min, and squares with dotted lines 12.5 μGy/min.

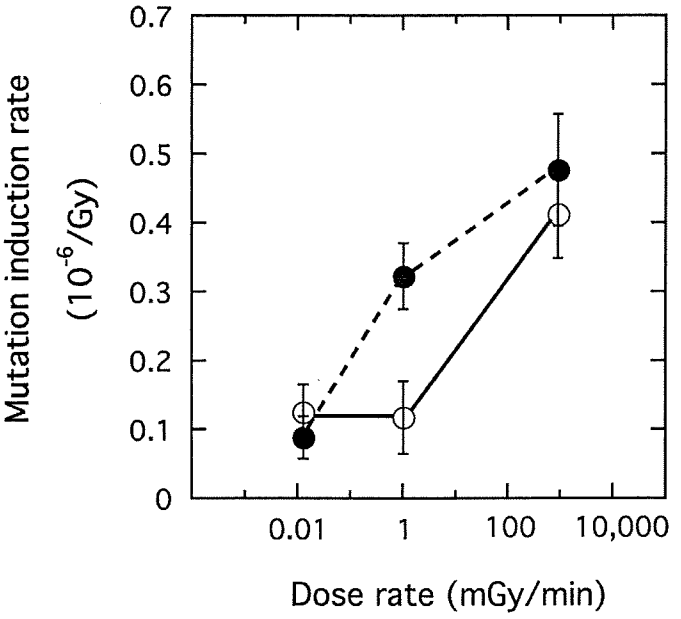

FIG. 2. Dose-rate dependence of the radiation-induced mutation rate in the *red-gam* genes. The slopes of the lines in Fig. 1 were analyzed by linear regression and plotted as a function of the dose rate. The open circles with solid lines indicate the liver, and the closed circles with dotted lines indicate the spleen. The vertical lines indicate standard errors of the slopes. The mutation induction rates in spleen and liver at 1 mGy/min are statistically significantly different (P = 0.0037).

primers surrounding one terminal of the inserted sequence at its original location. The positions of the primers were at 4476–4496 (21 mer) and 6638–6658 (21 mer) in lambda EG10.

Statistical Analysis

The statistical analyses were performed using StatView 5.0 software (http://www/hulinks.co.jp/software/statview). Mutant frequencies were analyzed with the t test. The dose–response curves of mutation induction were examined by regression analyses. The variations in the dose responses under different dose rates as well as between the spleen and liver were analyzed by ANCOVA. Occurrences of different types of mutations were analyzed with the contingency test. In all cases, a P value of less than 0.05 was considered to be a statistically significant difference.

RESULTS

Mutations Induced by Radiation Delivered at Different Dose Rates

Mutation frequencies observed after irradiation with different doses of high- (920 mGy/min), medium- (1 mGy/min) and low-dose-rate (12.5 μGy/min) γ rays in the spleens and livers of *gpt* delta mice are shown in Fig. 1. The mutant frequencies for each individual mouse is shown in Supplementary Tables S1 and S2. In control nonirradiated mice, slight increases in mutation frequency were observed between 2 and 18 months of age in the two tissues. The increase in the spleen was from (1.083 ± 0.180) × 10^{-6} (4 mice) to (1.783 ± 0.492) × 10^{-6} (9 mice), and the difference was statistically significant with a P value of 0.0033. The slight increase in the liver was not statistically significant (P = 0.243). After 2 to 8 Gy of high- or medium-dose-rate radiation, a linear increase in the mutant frequency was observed in the two tissues. The linear regression analyses of the results showed the relationships between mutant frequency (×10^{-6}) and dose (in Gy) as follows: mutant frequency 1.11 + (0.477 ± 0.081)D, r = 0.871 for high-dose-rate spleen, 1.14 + (0.323 ± 0.048)D, r = 0.922 for medium-dose-rate spleen, 0.743 + (0.413 ± 0.064)D, r = 0.917 for high-dose-rate liver, and 1.364 + (0.118 ± 0.053)D, r = 0.643 for medium-dose-rate liver. The mutant frequencies after irradiation with the low dose rate (12.5 μGy/min) were (2.496 ± 0.610) × 10^{-6} (10 mice) in spleen and (2.560 ± 0.808) × 10^{-6} (10 mice) in liver, whereas the levels in age-matched control mice were (1.783 ± 0.492) × 10^{-6} (9 mice) in spleen and (1.553 ± 0.424) × 10^{-6} (8 mice) in liver. The differences between the 18-month-old nonirradiated control mice and the irradiated mice were statistically significant in both spleen (P = 0.0128) and liver (P = 0.0043). The linear regression analyses of these data showed the following relationships: mutant frequency = 1.78 + (0.089 ± 0.031)D, r = 0.572 for spleen and 1.554 + (0.126 ± 0.040)D, r = 0.622 for liver.

The slopes of the dose–response regression lines were plotted as a function of the dose rate in Fig. 2. The mutation induction rate in spleen was different between the high and low dose rate (P = 0.0002) and between the medium and low dose rate (P = 0.0370) but not between the high and medium dose rate (P = 0.14). In the liver,

the mutation induction rate with high-dose-rate radiation was different from medium- and low-dose-rate radiation at statistically significant levels, $P = 0.0024$ and 0.0035, respectively. The mutation induction rates at 1 mGy/min and 12.5 μGy/min were similar. When the mutation induction rates in spleen and liver were compared, a statistically significant difference was found for medium dose rate ($P = 0.0037$) but not for high or low dose rate.

Molecular Nature of Radiation-Induced Mutations

In an attempt to determine whether specific types of mutations were induced by high- and low-dose-rate irradiation, 26 to 38 mutant clones were collected randomly from three mice from each experimental group and the DNA was sequenced. Some mutants showed identical alterations to other mutants isolated from the same DNA sample. These mutants were eliminated from counting because they were likely to have represented mutated DNA produced through replication of DNA and may not have reflected original mutations. The total number of original mutants sequenced was 236. All of the mutant clones showed deletion mutations in the *gam* gene, except for two clones that showed base substitutions in the *gam* gene and deletions or tandem mutations in the *red* gene.

The original mutants were classified into six groups: 1-bp deletion, 2–1,000-bp deletion, more than 1,000-bp deletion, insertions, multiple mutations, and complex mutations. A multiple mutation was defined as two or more mutations in separate positions in the *red-gam* gene or in its neighboring region. Complex mutations included all kinds of mutations that were not included in the former groups. They could be explained by the simultaneous occurrence of a deletion and insertion in one location. The percentages of each type of mutation found in irradiated and nonirradiated mice are shown in Fig. 3. In nonirradiated mice, in both tissues, the 1-bp deletions were dominant followed by the deletion of more than 1,000 bp. This pattern was similar even as the mice aged (up to 18 months). In irradiated mice, the fraction of 2-bp to 1-kbp deletions was elevated regardless of tissue or mode of irradiation. The elevation in mutations after high-dose-rate irradiation with 4 Gy in spleen and 8 Gy in liver and after low-dose-rate irradiation in the spleen with a total dose of 8 Gy were statistically significant at the level of $P = 0.0232$, 0.000745 and 0.0128, respectively. The elevation in the spleen after a high-dose-rate 8-Gy irradiation and in the liver after a low-dose-rate irradiation were not statistically significant, with P values of 0.054 and 0.11, respectively. These results suggest that deletion mutations of 2 to 1,000 bp are induced by radiation. No significant difference in the mutation spectra after high- or low-dose-rate irradiation were found.

Other types of mutations such as insertions and multiple and complex mutations were not frequent. The exact sequence changes found in the multiple and complex mutations are listed in Table 2. All 11 complex mutations could be explained by the simultaneous occurrence of a deletion and an insertion in one place. Eleven out of 14 multiple mutations showed two mutations in separate positions. Some of these included complex mutations and tandem mutations. The remaining three multiple mutations were more complicated. Clone 18L6-10 from the liver of a chronically irradiated mouse showed two base substitutions and one base deletion in nearby locations (Table 2). These mutations could also be explained by a 5-bp deletion of 25,100–25,104 and a simultaneous insertion of AG. In that case, this clone should be classified as a complex type mutation. The clone 18L2-1 found in the liver of an old nonirradiated mouse showed five base substitutions and one large deletion of –7,664 bp. Three of the five base substitutions were located at 29, 20 and 13 bp from the left end terminal of the deletion. The other two base substitutions were located at 238 and 828 bp from the right end of deletion. All five base substitutions were G:C to A:T transitions. The third multiple mutation was one found in the spleen of a high-dose-rate-irradiated mouse, 2S4-5, exposed to 8 Gy. This showed two base substitutions at 36,025 and 38,876 together with a complex mutation at a distant site. The complex mutation was composed of an 8,936-bp deletion (24,136 to 33,071) and a 6,139-bp insertion in the same location. Most of the inserted sequence, 6,136 bp out of 6,139 bp, showed homology to another part of lambda EG10 (12 to 6,147) in an inverted direction. At the left end junction of the deletion and insertion, an extra insertion of ACA was observed. These alterations are illustrated in Fig. 4. The presence of the original sequence of 12 to 6,147 bp was confirmed at the correct position in the mutant clone with PCR by using primers located at the upstream and downstream sides of 6,147. Thus the inserted sequence must have been duplicated from the original sequence rather than translocated.

DISCUSSION

The present study shows that the mutagenic effects of radiation in somatic tissues depend on both the dose rate and the tissue. In the liver, the efficiency of mutation induction was reduced from 0.41×10^{-6}/Gy to 0.12×10^{-6}/Gy when the dose rate was reduced from 920 mGy/min to 1 mGy/min, but it remained at a similar level when the dose rate was reduced further to 12.5 μGy/min (0.13×10^{-6}/Gy). The efficiency at high dose rates was similar to that observed previously with 0.77 Gy/min of X rays using *gpt* delta mice (*18*). The dose-rate dependence resembled the previous observations made in spermatogonia (*3, 4*), splenic T cells (*1*), and intestinal

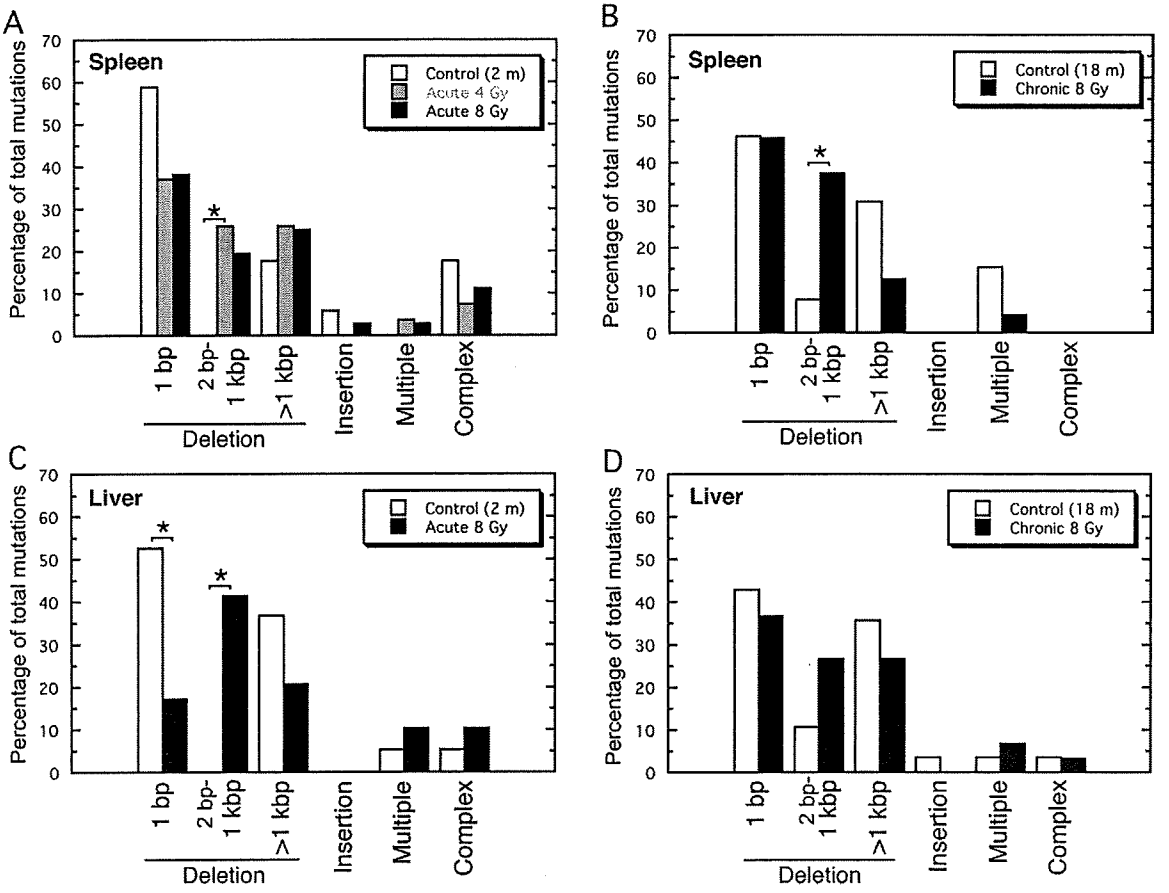

FIG. 3. Frequencies of different types of mutations in control and irradiated mice. Deletion mutations were classified into three groups according to the size of deleted fragments: 1 bp, 2 bp–1 kbp and more than 1 kbp. The incidence of each type of mutation among the non-redundant mutations was calculated. Open bars indicate unirradiated age-matched control mice while the gray and black bars show 4-Gy-irradiated and 8-Gy-irradiated mice, respectively. Panel A: Spleen with or without high-dose-rate irradiation with 4 Gy or 8 Gy. Panel B: Spleen with or without low-dose-rate irradiation with 8 Gy. Panel C: Liver with or without high-dose-rate irradiation with 8 Gy. Panel D: Liver with or without low-dose-rate irradiation with 8 Gy. The percentages of 2- bp–1-kbp deletions were elevated after irradiation. Asterisks show statistically significant differences between control and irradiated mice.

stem cells (*2*). In spleen, on the other hand, the efficiency decreased steadily from 0.48×10^{-6}/Gy to 0.089×10^{-6}/Gy as the dose rate was reduced from 920 mGy/min to 12.5 μGy/min. The efficiency was higher in spleen than in liver when the dose rate was 1 mGy/min but was similar at 920 mGy/min and 12.5 μGy/min (Fig. 2).

The reduction of the mutation induction rate observed when the dose rate decreased from 1 mGy/min to 12.5 μGy/min in spleen does not agree with a previous study on splenic T lymphocytes in which *Hprt* mutation rates showed a dose-rate effect between 500 mGy/min and 0.69 mGy/min but no further reduction at 99 μGy/min (*1*). This discrepancy might be explained by an underestimation of the *Hprt* mutation frequency, especially with low-dose-rate exposures, because the *Hprt* mutant frequency is reported to decline with time (*1*). For low-dose-rate irradiation, the mutations induced at early stages might be eliminated if the assays were performed at long times after the beginning of the irradiation.

In the present study, the dose–response curves were estimated to be linear for the three dose rates examined. Linearity was also observed for mutagenic effects in germ-line cells (*4*). On the other hand, many other genetic effects, including chromosome abnormalities, had linear-quadratic dose responses (*22*). Thus the dose response of mutagenic effects could also be linear-quadratic rather than linear. Because the data obtained in our study were limited, it is difficult to determine whether the dose–response relationship for the mutagenic effects were linear or linear-quadratic (Fig. 1, Supplementary Tables S1, S2).

The low dose rate we adopted was 12.5 μGy/min, and the irradiation continued for 483 days. Under these conditions, many of the mutations observed would reflect mutations accumulated in stem cells, especially in spleen, which is a cell-proliferating tissue. The high and medium dose rates, on the other hand, were 920 mGy/min and 1 mGy/min and continued for 8.7 min and 5.56 days to reach to total dose of 8 Gy, respectively. The

TABLE 2
Unusual Mutations

Tissue	Age (months)	Dose (Gy)[a]	Mutant number	Position	Change[b]	Class[c]
Spleen	2	4	2S1-6	24,987–24,997	GCCA···CTGA → GC(G)GA (–11+1)	C
			2S2-7	25,054–25,055	GGCGTT → GG(T)TT (–2+1)	C
			2S3-1	25,102	GGCCT → GGGCT	M
				25,108	CCTTTTTCC → CCTTTTCC (–1)	
		8	2S4-5	24,136–33,071	GCCA···TTAC → GC(AC···GA)GG (–8,936+6139)	C,M
				36,025	AACCA → AATCA	
				38,876	GATAA → GAATT	
			2S6-2	24,981–24,983	TGTTCTG → TG(GG)TG (–3+2)	C
			2S6-6	24,513–25,284	GCGA···AGGG → GC(AA)GG (–772+2)	C
			2S6-8	25,016–25,017	ATCAAA → AT(T)AA (–2+1)	C
	18	0	18S1-12	23,942	CAGC → CA(CA···CA)GC (+17)	M
				24,730–26,052	TCTT···ACAC → TCAC (–1,323)	
			18S2-12	20,075	AGAT → AG(TC···AG)AT (+28)	M
				20,345–26,215	ACCA···TTGG → ACGG (–5,870)	
			18S3-1	21,208	AGAAA → AGGAA	M
				21,581–25,835	TGGG···CAGT → TG(T)GT (–4,255+1)	C
			18S3-6	24,511–25,737	GCAG···GCTT → GCTT (–1,227)	M
				25,762	GCGCG → GCACG	
		8(crh)	18S5-12	23,700–24,828	CGAG···AGTG → CGTG (–3,979)	M
				25,075	ATAGC → ATCGC	
Liver	2	0	2L2-1	24,943–24,944	CCTGGT → CC(A)GT (–2+1)	C
			2L3-8	25,049	CCCGT → CCGT (–1)	M
				32,876–39,221	TCCC···TCTG → TCTG (–6,297)	
		8	2L4-9	25,055–25,057	GCGTTGC → GC(TG)GC (–3+2)	C
			2L4-12	24,948–24,949	TGGTGA → TGAAGA	T,M
				24,955–24,967	CAAT···CATG → CATG (–13)	
			2L6-3	25,019	AAACG → AACG (–1)	M
				26,083	TGGTT → TGTTT	
			2L6-5	24,983	TTCTG → TTTG (–1)	M
				25,147	GGGCG → GGTCG	
			2L6-10	23,514–25,232	TGAA···TAGC → TG(CT)GC (–1,719+2)	C
	18	0	18L1-4	24,902–25,002	GTGC···ACTC → GT(AA)TC (–101+2)	C
			18L2-1	23,894	CAGGC → CAAGC	M
				23,902	TGCTT → TGTTT	
				23,908	AGCGT → AGTGT	
				23,925–31,588	CCAC···TGTA → CCTA(–7,664)	
				31,825	CGGCG → CGACG	
				32,414	TGCAG → TGTAG	
	18	8(chr)	18L6-2	24,760–24,761	TTGGCA → TTTTCA	T,M
			18L6-6	25,017	TCAAA → TCTAA	
			18L6-10	25,056–25,820	CGTT···TGGT → CG(A)GT (–765+1)	C
				25,100	CAGGC → CAAGC	M
				25,103	GCCTT → GCGTT	
				25,108	CCTTTTTCC → CCTTTTCC (–1)	

[a] (chr) indicates chronic irradiation at a dose rate of 12.5 μGy/min for 483 days.
[b] Altered sequences are underlined. Bases shown in parentheses indicate inserted bases. The numbers in parentheses show the size of deletions indicated by a minus sign, and the size of insertions indicated with a plus sign.
[c] Unusual mutation classes are C for complex, M for multiple, and T for tandem.

mutation frequency was assayed 1 week after the end of irradiation. The mutations observed under these conditions would represent mostly those in the progenitor cells and terminally differentiated cells rather than stem cells. Thus the differences in the mutation induction rates observed for medium- and low-dose-rate-irradiated spleen (Fig. 2) might reflect the different radiosensitivities of stem cells and progenitor/differentiated cells. However, this concept does not appear to be applicable to the liver, because the mutation induction rates were similar for medium- and low-dose-rate irradiation (Fig. 2) and because the cell proliferation rate in liver is very slow.

The dose-rate effect evaluated by the mutation induction rate for 920 mGy/min divided by that for 12.5 μGy/min was 5.4 for spleen (0.477/0.089) and 3.3 for liver (0.413/0.126) (Fig. 2). These values corresponded roughly to the dose-rate effects for tumor induction in many mouse tissues examined in the past, which varied from 2 to 11 depending on tissue, strain of mouse,

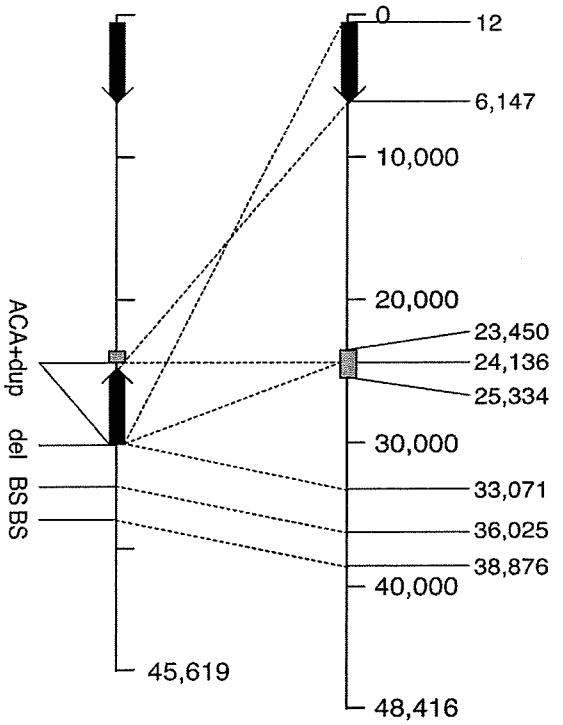

FIG. 4. Schematic illustration of the lambda EG10 genome showing the intricate mutations found in the liver of an aged control mouse. The right vertical line indicates the lambda EG10 genome, and the numbers show the positions in base pairs from the cos site. The left vertical line shows mutated lambda EG10. Gray squares in the middle show the *red-gam* genes before and after the mutation event. Bold black arrows indicate the sequence of lambda EG10 located between 12 and 6,147. In the mutant DNA, five alterations were found: two base substitutions at bp 36,025 and 38,876, deletion of base pairs from 24,136 to 33,071, duplication and insertion of 12 to 6,147 bp at 24,136; and insertion of an ACA sequence at the upper terminal of the duplicated fragment.

sex, etc. (*23*). Although the dose-rate effects specific for spleen and liver tumor induction in the mouse strain we used are not available, the similarity of the dose-rate effects in mutation induction and tumor induction may support the idea that mutation induction is closely related to radiation carcinogenesis.

Analysis of the molecular nature of mutations using DNA sequencing revealed that the predominant type of mutation observed was a deletion of 1 to 8,112 bp in both nonirradiated and irradiated mice. Among these deletions, the frequency of medium-size deletions of 2 to 1,000 bp was elevated in irradiated tissues (Fig. 3), indicating that they were induced by radiation. Similar results have been observed previously in the spleen (*17*). The fraction of large deletion of more than 1 kbp showed similar levels in spleen before and after acute irradiation with 4 and 8 Gy (Fig. 3A), whereas the fraction decreased after low-dose-rate irradiation (Fig. 3B), although the difference was not statistically significant ($P = 0.0697$). This may suggest that the occurrence of large deletions is suppressed after low-dose-rate irradiation compared to high-dose-rate irradiation. A similar phenomenon was reported in cultured cells (*7*). A slight reduction of large deletions was also observed in liver (Fig. 3C). In this tissue, however, the trend of reduction after irradiation was observed after high-dose-rate irradiation but not after low-dose-rate irradiation (Fig. 3D). This may suggest a tissue difference in radiation-induced mutation between spleen and liver.

Studies in yeast have revealed three kinds of DNA repair systems that generate deletion-type mutations, non-homologous end joining (NHEJ), microhomology-mediated end joining (MMEJ), and single-strand annealing (SSA), which function in the repair of DNA double-strand breaks (*24, 25*). One of the major characteristics of these repair systems is the difference in size of the homologous sequences that are used in the ligation through annealing of the separated DNA ends generated by a double-strand break. They were 1 to 4 nucleotides in NHEJ, 5 to 20 nucleotides in MMEJ, and more than 20 nucleotides in SSA (*24*). Similar phenomena were observed in chicken and mammalian cells (*25, 26*). Thus, in the work described here, homologous sequences near the termini of the deletion mutations were examined and grouped into three classes depending on the size of the homologous sequences at the break points 0, 1–4 and 5 or more. The 0-bp homology class was considered as a separate group because this kind of deletion was observed previously to be elevated by radiation (*14–17*). The maximum size of the homologies observed in the present experiment was 12 nucleotides; homologies of more than 20 nucleotides, which correspond to SSA, were not found. The percentages of each kind of mutation among the total number of deletion mutations are shown in Fig. 5. Deletions in the multiple and complex mutations were not included. The percentage of zero homology was elevated in spleen after 8 Gy high-dose-rate irradiation (Fig. 5A) ($P = 0.0443$). The increase was accompanied by a decrease in 5 or more nucleotide homologies. This may suggest that the contribution of MMEJ is small during repair of radiation-induced DNA double-strand breaks, at least in the spleen. An increase of deletions without homologous terminal sequences was also observed in the liver after 8 Gy acute irradiation (Fig. 5C), although the difference was not statistically significant ($P = 0.0964$). The frequencies of deletions with 1–4-bp homology did not change much among the samples. When all of the mutations found in control and irradiated mice were summed up, the frequency of deletions containing 5 or more bases of terminal homology appeared to be higher in the spleen than in the liver. These events comprised 30 out of 114 deletion mutations in the spleen and only 10 out of 92 deletion mutations in the liver ($P = 0.00533$). Thus it is likely that the contribution of MMEJ is higher in the spleen than in the liver. This is in agreement with the fact that MMEJ works more efficiently in the S and

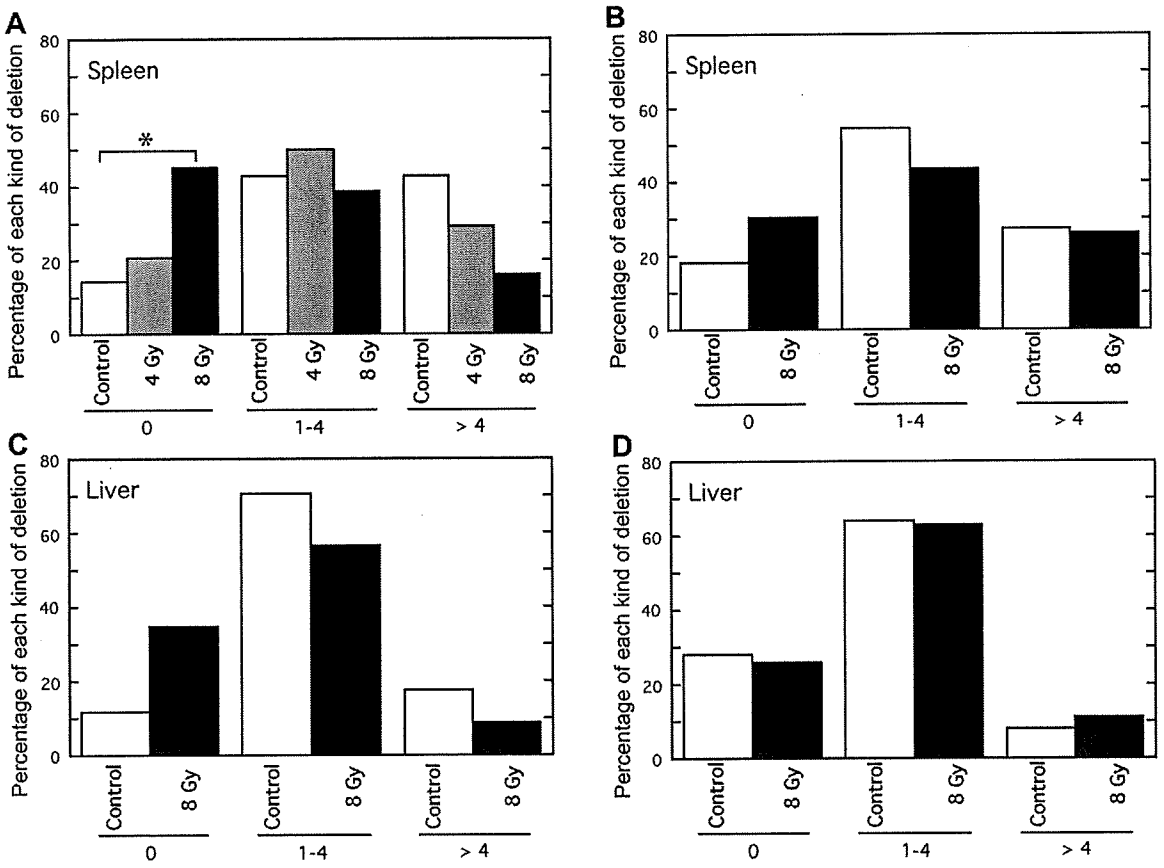

FIG. 5. Comparisons of the frequencies of deletion mutations showing repeated sequences of different sizes at the junctions of the deletions. The deletions were classified into three groups: no homology at the junction, 1 to 4-bp-long homology, and 5-bp-long or more homology. The frequency of each group of mutations was calculated for spleen (panel A) and liver (panel C) in high-dose-rate-irradiated mice and in the spleen (panel B) and liver (panel D) of low-dose-rate-irradiated mice. Statistically significant differences are indicated by an asterisk.

G_2 phases of the cell cycle (*24, 25*), because the spleen is a tissue in which many cells are dividing and are therefore in S and G_2 phase, whereas the liver contains almost exclusively slowly dividing cells in the G_0 or G_1 phase.

Among the 236 non-redundant mutations found in the present study, 14 were multiple mutations. This frequency of 5.9×10^{-2} (14/236) was much higher than the expected value for the coincidental occurrence of two or more single mutations, because the expected frequency of a single mutation was of the order of 10^{-6}. The mutation frequency observed was 1 to 5×10^{-6} (Fig. 1), and most of these (222 out of 236) were single mutations. This high frequency of multiple mutations was observed in many other systems (*27*), including normal tissues of the Big-Blue mouse (*28*) and the epithelial tissues in the intestines of aged Muta™ mice (*29*). A possible mechanism that could explain the production of these multiple mutations could be the involvement of some trans-lesional DNA polymerases, which replicate DNA with an extremely high error rate and can result in two or more mutations within a DNA stretch only several kbp long (*30–33*).

To understand how these multiple mutations were generated, it would be helpful to scrutinize their molecular nature. Among the 14 multiple mutations, 13 showed changes in DNA length including deletions, insertions and complex-type mutations. One exception was a base substitution in the *gam* gene and a tandem base substitution in the *red* gene (18L6-2). Frequent associations of deletion mutations and other types of mutations in nearby positions along a single DNA strand have been reported in two cases: a preferential occurrence of base substitution mutations in the *Ki-ras* proto-oncogene allele containing 37 base deletions in the second intron (*34*) and a high rate of single nucleotide mutations in the areas neighboring deletion and insertion mutations in evolutionary changes (*35*). Although the molecular mechanisms of these phenomena have not been elucidated, a possible association with error-prone trans-lesional DNA polymerases in MMEJ is one possibility (*25*).

The mutant clone 18L2-1 found in the liver of an aged control mouse (Table 2) had one deletion of –7,664 bp together with 5 base substitutions in the neighboring area. All of the 5 base substitutions were G:C to A:T transition mutations. This could be induced by an imbalance in the pool size of deoxyribonucleotide triphosphates. In cultured cells, an increase of the dTTP pool size has been shown to result in the induction of

G:C to A:T transition mutations (*36, 37*). The clustering of the base substitutions in the nearby regions of the deletion mutation may suggest that the pool size effect becomes more effective when DNA polymerization takes place together with a deletion mutation. The deletion mutation found in this clone did not have any homologous sequences at the terminals, suggesting that it was not generated by MMEJ or SSA.

In conclusion, the mutagenic effects of radiation in spleen and liver were shown to be dependent on the dose rate. The detail information about the mutation induction rates as well as the molecular characteristics of mutations revealed some differences between the two tissues. Further studies on the other tissues would be important to understand dose-rate effects at the organismal level.

SUPPLEMENTARY INFORMATION

Tables S1 and S2. Mutant frequencies in spleen and liver, respectively, of each individual mouse. http://dx.doi.org/10.1667/RR1932.1.S1

ACKNOWLEDGMENTS

We thank Y. Ikeda and Y. Syono for their technical assistance and Dr. L. N. Kapp for editorial help. This study was partially supported by the Budget for Nuclear Research of the Ministry of Education, Culture, Sports, Science and Technology, based on the screening and counseling by the Atomic Energy Commission. The study was partially supported by the NIFS Collaborative Research Program (NIFS07KOBS012) and also partially supported by a contract with the Aomori Prefectural Government, Japan.

Received: July 17, 2009; accepted: October 1, 2009

REFERENCES

1. R. Lorenz, W. Deubel, K. Leuner, T. Göllner, E. Hochhäuser and K. Hempel, Dose and dose-rate dependence of the frequency of HPRT deficient T lymphocytes in the spleen of the ^{137}Cs gamma-irradiated mouse. *Int. J. Radiat. Biol.* **66**, 319–326 (1994).
2. D. J. Winton, J. H. Peacock and B. A. J. Ponder, Effect of gamma radiation at high- and low-dose rate on a novel in vivo mutation assay in mouse intestine. *Mutagenesis* **4**, 404–406 (1989).
3. M. F. Lyon, D. G. Papworth and R. J. S. Phillips, Dose-rate and mutation frequency after irradiation of mouse spermatogonia. *Nat. New Biol.* **238**, 101–104 (1972).
4. W. L. Russell and E. M. Kelly, Mutation frequencies in male mice and the estimation of genetic hazards of radiation in men. *Proc. Natl. Acad. Sci. USA* **79**, 542–544 (1982).
5. A. Shimada, H. Eguchi, S. Yoshinaga and A. Shima, Dose-rate effect on transgenerational mutation frequencies in spermatogonial stem cells of the medaka fish. *Radiat. Res.* **163**, 112–114 (2005).
6. K. J. Sorensen, L. A. Zetterberg, D. O. Nelson, J. Grawe and J. D. Tucker, The *in vivo* dose rate effect of chronic gamma radiation in mice: translocation and micronucleus analyses. *Mutat. Res.* **457**, 125–136 (2000).
7. H. Nakamura, H. Fukami, Y. Hayashi, A. Tachibana, S. Nakatsugawa, M. Hamaguchi and K. Ishizaki, Cytotoxic and mutagenic effects of chronic low-dose-rate irradiation on *TERT*-immortalized human cells. *Radiat. Res.* **163**, 283–288 (2005).
8. P. R. V. Kumar, M. N. Mohankumar, V. Z. Hamza and R. K. Jeevanram, Dose-rate effect on the induction of *HPRT* mutants in human G_0 lymphocytes exposed *in vitro* to gamma radiation. *Radiat. Res.* **165**, 43–50 (2006).
9. M. M. Vilenchik and A. G. Knudson, Inverse radiation dose-rate effects on somatic and germ-line mutations and DNA damage rates. *Proc. Natl. Acad. Sci. USA* **97**, 5381–5386 (2000).
10. M. M. Vilenchik and A. G. Knudson, Radiation dose-rate effects, endogenous DNA damage, and signaling resonance. *Proc. Natl. Acad. Sci. USA* **103**, 17874–17879 (2006).
11. K. Tanaka, A. Kohda, K. Satoh, T. Toyokawa, K. Ichinohe, M. Ohtaki and Y. Oghiso, Dose-rate effectiveness for unstable-type chromosome aberrations detected in mice after continuous irradiation with low-dose-rate gamma rays. *Radiat. Res.* **171**, 290–301 (2009).
12. J. Vijg and H. van Steeg, Transgenic assays for mutations and cancer: current status and future perspectives. *Mutat. Res.* **400**, 337–354 (1998).
13. T. Nohmi, M. Katoh, H. Suzuki, M. Matsui, M. Yamada, M. Watanabe, M. Suzulki, N. Horiya, O. Ueda and T. Sofuni, A new transgenic mouse mutagenesis test system using Spi$^-$ and 6-thioguanine selections. *Environ. Mol. Mutagen.* **28**, 465–470 (1996).
14. T. Nohmi and K. Masumura, *Gpt* delta transgenic mouse: a novel approach for molecular dissection of deletion mutations *in vivo*. *Adv. Biophys.* **38**, 97–121 (2004).
15. T. Ono, H. Ikehata, S. Nakamura, Y. Saito, J. Komura, Y. Hosoi and K. Yamamoto, Molecular nature of mutations induced by a high dose of X-rays in spleen, liver, and brain of the lacZ-transgenic mouse. *Environ. Mol. Mutagen.* **34**, 97–105 (1999).
16. Y. Uehara, H. Ikehata, J. Komura, A. Ito, M. Ogata, T. Itoh, R. Hirayama, Y. Furusawa, K. Ando and T. Ono, Absence of Ku70 gene obliterates X-ray-induced lacZ mutagenesis of small deletions in mouse tissues. *Radiat. Res.* **170**, 216–223 (2008).
17. T. Nohmi, M. Suzuki, K. Masumura, M. Yamada, K. Matsui, O. Ueda, H. Suzuki, M. Katoh, H. Ikeda and T. Sofuni, Spi$^-$ selection: an efficient method to detect gamma-ray-induced deletions in transgenic mice. *Environ. Mol. Mutagen.* **34**, 9–15 (1999).
18. I. Furuno-Fukushi, K. Masumura, T. Furuse, Y. Noda, M. Takahagi, T. Saito, Y. Hoki, H. Suzuki, A. Wynshaw-Boris and K. Tatsumi, Effect of *Atm* disruption on spontaneously arising and radiation-induced deletion mutations in mouse liver. *Radiat. Res.* **160**, 549–558 (2003).
19. P. M. Shaver-Walker, C. Urlando, K. S. Tao, X. B. Zhang and J. A. Heddle, Enhanced somatic mutation rates induced in stem cells of mice by low chronic exposure to ethylnitrosourea. *Proc. Natl. Acad. Sci. USA* **92**, 11470–11474 (1995).
20. S. Tanaka, I. B. Tanaka, III, S. Sasagawa, K. Ichinohe, T. Takabatake, S. Matsushita, T. Matsumoto, H. Otsu and F. Sato, No lengthening of life span in mice continuously exposed to gamma rays at very low dose rates. *Radiat. Res.* **160**, 376–379 (2003).
21. I. B. Tanaka, III, S. Tanaka, K. Ichinohe, S. Matsushita, T. Matumoto, H. Otsu, Y. Oghiso and F. Sato, Cause of death and neoplasia in mice continuously exposed to very low dose rates of gamma rays. *Radiat. Res.* **167**, 417–437 (2007).
22. National Research Council Committee on Health Risks from Exposure to Low Levels of Ionizing Radiation, *Health Risks from Exposure to Low Levels of Ionizing Radiation: BEIR VII Phase 2*. National Academies Press, Washington, DC, 2006.
23. UNSCEAR, *Sources and Effects of Ionizing Radiation*. United Nations, New York, 1993.
24. K. Lee and S. E. Lee, *Saccharomyces cerevisiae* Sae2- and Tell-dependent single-strand DNA formation at DNA break pro-

motes microhomology-mediated end joining. *Genetics* **176**, 2003–2014 (2007).

25. M. McVey and S. E. Lee, MMEJ repair of double-strand breaks (director's cut): deleted sequences and alternative endings. *Trends Genet.* **24**, 529–438 (2008).
26. M. H. Yun and K. Hiom, CtIP-BRCA1 modulates the choice of DNA double-strand-break repair pathway throughout the cell cycle. *Nature* **450**, 509–514 (2007).
27. J. W. Drake, A. Bebenek, G. E. Kissling and S. Peddada, Clusters of mutations from transient hypermutability. *Proc. Natl. Acad. Sci. USA* **102**, 12849–12854 (2005).
28. J. Wang, K. D. Gonzalez, W. A. Scaringe, K. Tsai, N. Liu, D. Gu, W. Li, K. A. Hill and S. S. Sommer, Evidence for mutation showers. *Proc. Natl. Acad. Sci. USA* **104**, 8403–8408 (2007).
29. T. Ono, H. Ikehata, V. P. Pithani, Y. Uehara, Y. Chen, Y. Kinouchi, T. Shimosegawa and Y. Hosoi, Spontaneous mutations in digestive tract of old mice show tissue-specific patterns of genomic instability. *Cancer Res.* **64**, 6919–6923 (2004).
30. B. D. Harfe and S. Jinks-Robertson, DNA polymerase zeta introduces multiple mutations when bypassing spontaneous DNA damage in *Saccharomyces cerevisiae*. *Mol. Cell* **6**, 1491–1499 (2000).
31. T. Matsuda, K. Bebenek, C. Masutani, I. B. Rogozin, F. Hanaoka and T. A. Kunkel, Error rate and specificity of human and murine DNA polymerase eta. *J. Mol. Biol.* **312**, 335–346 (2001).
32. X. Zhong, P. Garg, C. M. Stith, S. A. Nick McElhinny, G. E. Kissling, P. M. J. Burgers and T. A. Kunkel, The fidelity of DNA synthesis by yeast DNA polymerase zeta alone and with accessory proteins. *Nucleic Acids Res.* **34**, 4731–4742 (2006).
33. S. D. McCulloch, R. J. Kokoska, P. Garg, P. M. Burgers and T. A. Kunkel, The efficiency and fidelity of 8-oxo-guanine bypass by DNA polymerases delta and eta. *Nucleic Acids Res.* **37**, 2830–2840 (2009).
34. M. You, Y. Wang, G. Stoner, L. You, R. Maronpot, S. H. Reynolds and M. Anderson, Parental bias of Ki-*ras* oncogenes detected in lung tumors from mouse hybrids. *Proc. Natl. Acad. Sci. USA* **89**, 5804–5808 (1992).
35. D. Tian, Q. Wang, P. Zhang, H. Araki, S. Yang, M. Kreitman, T. Nagylaki, R. Hudson, J. Bergelson and J-Q. Chen, Single-nucleotide mutation rate increases close to insertions/deletions in eukaryotes. *Nature* **455**, 105–108 (2008).
36. G. Phear and M. Meuth, A novel pathway for transversion mutation induced dCTP misincorporation in a mutator strain of CHO cells. *Mol. Cell. Biol.* **9**, 1810–1812 (1989).
37. E. Darè, L-H. Zhang, D. Jenssen and V. Bianchi, Molecular analysis of mutations in the *hprt* gene of V79 hamster fibroblasts: effects of imbalances in the dCTP, dGTP and dTTP pools. *J. Mol. Biol.* **252**, 514–521 (1995).

Genes and Environment, Vol. 31, No. 3 pp. 69-79 (2009)

Regular article

Development of Tester Strains Deficient in Nth/Nei DNA Glycosylases to Selectively Detect the Mutagenicity of Oxidized DNA Pyrimidines

Masami Yamada, Keiko Matsui, Atsushi Katafuchi, Makiko Takamune and Takehiko Nohmi[1]

Division of Genetics and Mutagenesis, National Institute of Health Sciences, Tokyo, Japan

(Received April 22, 2009; Revised May 30, 2009; Accepted June 9, 2009)

Oxidative DNA damage is a major cause of mutation and cell death in aerobic organisms. In addition to 8-hydroxyguanine, oxidized DNA pyrimidines play important roles in mutagenesis. *Salmonella typhimurium* TA1535, widely used in mutagenicity assays, carries a *hisG46* missense mutation and efficiently detects mutations at G:C base pairs. To detect oxidative mutagens that selectively modify pyrimidines, we constructed a derivative of strain TA1535, termed YG3206, which lacks the Nei and Nth DNA glycosylases that excise oxidized pyrimidines from DNA. This novel strain easily detected the mutagenicity of L-cysteine, L-penicillamine, dopamine-HCl, and phenazine methosulfate, which are non-mutagenic or only weakly mutagenic in the TA1535 parent strain. A second strain that is equivalent to YG3206 but harbors the plasmid pKM101 which carries *mucAB* encoding DNA polymerase R1, termed YG3216, was significantly sensitive to phenazine ethosulfate. The compound was not mutagenic in either YG3206 or the Fapy-glycosylase-defective strain YG3001. Potassium bromate and methylene blue plus visible light with metabolic activation induced mutations in YG3001 but not YG3206 or YG3216. The number of spontaneous His$^+$ revertants per plate was 82 ± 16 (YG3206, *Δnth Δnei*), 19 ± 4 (YG3001, *Δfpg*), and 6 ± 2 (TA1535), suggesting a significant contribution to spontaneous mutagenesis by endogenous pyrimidine oxidation. In the absence of exogenous chemical treatment, exposure to fluorescent light enhanced the spontaneous mutation frequency by approximately two-fold (YG3206), 13-fold (YG3001), and 10-fold (TA1535). These results suggest that certain environmental chemicals may selectively introduce mutagenic damage at DNA pyrimidines, and that these changes can be monitored by the use of YG3206.

Key words: genotoxicity, oxidative damage, oxidized pyrimidines, Endo III, Endo VIII

Introduction

The DNA of all organisms is constantly damaged by endogenous processes, including oxidation, hydrolysis, and alkylation (1,2). A potential source of the large number of mutations produced during tumor progression is DNA damage, particularly damage by reactive oxygen species (ROS) (3). In aerobically grown cells, ROS are produced as by-products of normal metabolic pathways and have been shown to contribute to human diseases, including cancer, cardiovascular disease, immune system decline, and brain dysfunction (4). Some of the byproducts include singlet oxygen ($^1O_2$), peroxide radicals ($^{\cdot}O_2$), hydrogen peroxide (H_2O_2), and hydroxyl radicals ($^{\cdot}OH$) (5). The reactions mediated by ROS can lead to a wide variety of DNA damage, including DNA strand breaks, protein-DNA cross-links, abasic sites, and base lesions (6). Although cells possess many defenses against oxidative damage, it has been estimated that the mammalian genome undergoes roughly 10^4–10^5 oxidative attacks per day (4).

More than 50 different base lesions have been identified as the products of oxidative DNA damage (7). Arguably, the DNA base lesion receiving the most attention is 8-hydroxy-2′-deoxyguanosine (8-OH-dG, 7,8-dihydro-8-oxo-2′-deoxyguanosine), which is commonly used as a biomarker of oxidative DNA damage in the cell (8,9). When 8-OH-dG is present in a DNA template, A or C is inserted opposite 8-OH-dG, depending on the specific polymerase involved (10–12). In bacterial and mammalian cells, 8-OH-dG has been shown to produce high levels of G:C to T:A transversion mutations (13). In *Escherichia coli*, some enzymes are involved in processing 8-OH-dG-induced oxidative DNA damage (14). One enzyme is MutM glycosylase, or formamide pyrimidine DNA glycosylase (FPG), which is encoded by *mutM* or *fpg* and removes 8-hydroxyguanine (8-OH-G, 7,8-dihydro-8-oxoguanine) lesions found in DNA (15,16).

Oxidized pyrimidines also contribute mutations. For

[1]Correspondence to: Takehiko Nohmi, Division of Genetics and Mutagenesis, National Institute of Health Sciences, 1-18-1, Kamiyoga, Setagaya-ku, Tokyo 158-8501, Japan. Tel: +81-3-3700-9872, Fax: +81-3-3700-2348, E-mail: nohmi@nihs.go.jp